AD-A067 732 VANDERBILT UNIV NASHVILLE TN DEPT OF ELECTRICAL ENGI--ETC F/G 11/9
MICROWAVE CURING OF EPOXY RESINS.(U)
SEP 78 L K WILSON, J P SALERNO DAAG46-76-C-0035
UNCLASSIFIED USAAVRADCOM-TR-78-46 NL

1 OF 2
ADA
067732

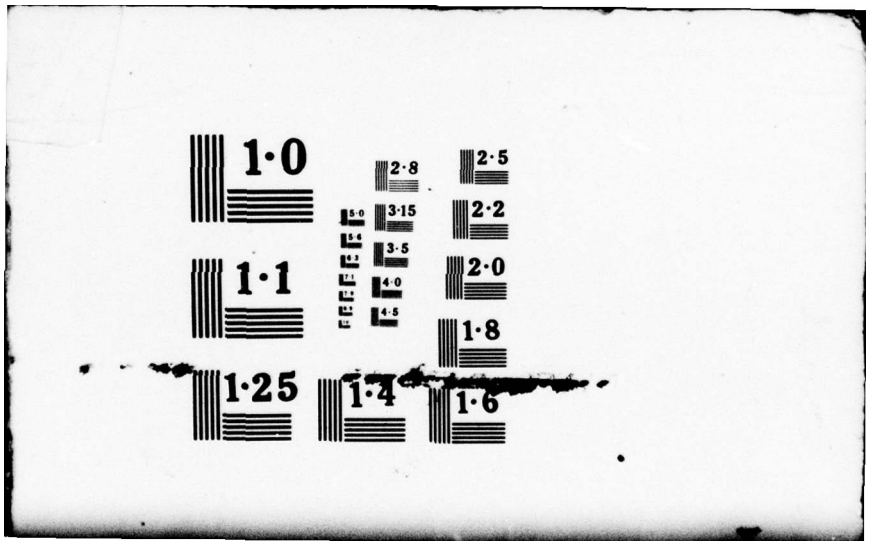
1·0
1·1
1·25
1·4
1·6
1·8
2·0
2·2
2·5
2·8
3·15
3·5
4·0
4·5

LEVEL II (12)

AD

AD A067732

DDC FILE COPY

AVRADCOM Report No. 78-46

# Production Engineering Measures Program Manufacturing Methods and Technology

# MICROWAVE CURING OF EPOXY RESINS

DDC RECEIVED APR 24 1979 C

L. K. WILSON AND J. P. SALERNO
VANDERBILT UNIVERSITY
NASHVILLE, TENNESSEE 37235

SEPTEMBER 1978

AMMRC TR 78-43

FINAL REPORT CONTRACT NUMBER DAAG46-76-C-0035

Approved for public release; distribution unlimited.

Prepared for
U.S. ARMY AVIATION SYSTEMS COMMAND
St. Louis, Missouri 63166

ARMY MATERIALS AND MECHANICS RESEARCH CENTER
Watertown, Massachusetts 02172

79 04 20 025

The findings in this report are not to be construed as an official Department of the Army position, unless so designated by other authorized documents.

Mention of any trade names or manufacturers in this report shall not be construed as advertising nor as an official indorsement or approval of such products or companies by the United States Government.

**DISPOSITION INSTRUCTIONS**

Destroy this report when it is no longer needed.
Do not return it to the originator.

SECURITY CLASSIFICATION OF THIS PAGE (When Data Entered)

## REPORT DOCUMENTATION PAGE

READ INSTRUCTIONS BEFORE COMPLETING FORM

1. REPORT NUMBER: AVRADCOM TR 78-46
2. GOVT ACCESSION NO.
3. RECIPIENT'S CATALOG NUMBER

4. TITLE (and Subtitle): Microwave Curing of Epoxy Resins
5. TYPE OF REPORT & PERIOD COVERED: Final Report
6. PERFORMING ORG. REPORT NUMBER: AMMRC FR 78-43

7. AUTHOR(s): L. K. Wilson, J. P. Salerno
8. CONTRACT OR GRANT NUMBER(s): DAAG46-76-C-0035

9. PERFORMING ORGANIZATION NAME AND ADDRESS:
Electrical Engineering Department
Vanderbilt University
Nashville, Tennessee 37235

10. PROGRAM ELEMENT, PROJECT, TASK AREA & WORK UNIT NUMBERS:
D/A Project: 1T37042
AMCMS Code: 1497.94.5.S7042
Agency Accession: (XL5)

11. CONTROLLING OFFICE NAME AND ADDRESS:
U. S. Army Aviation Systems Command
ATTN: DRSAV-EXT, P. O. Box 209
St. Louis, Missouri 63166

12. REPORT DATE: Sept[illegible]78
13. NUMBER OF PAGES: 113 p.

14. MONITORING AGENCY NAME & ADDRESS (if different from Controlling Office):
Army Materials and Mechanics Research Center
Watertown, Massachusetts 02172

15. SECURITY CLASS. (of this report): Unclassified
15a. DECLASSIFICATION/DOWNGRADING SCHEDULE

16. DISTRIBUTION STATEMENT (of this Report):
Approved for public release; distribution unlimited.

17. DISTRIBUTION STATEMENT (of the abstract entered in Block 20, if different from Report):
USAAVRADCOM, AMMRC

18. SUPPLEMENTARY NOTES
TR-78-46, TR-78-43

19. KEY WORDS (Continue on reverse side if necessary and identify by block number)

Epoxy resins
Curing
Dielectric Properties
Dielectric heating
Microwaves

20. ABSTRACT (Continue on reverse side if necessary and identify by block number)

This work is an investigation of the mechanisms responsible for the microwave heating behavior of epoxies as applied to the cure of fiberglass/Epoxy laminate structures. The problem is approached by the derivation of a mathematical relation for the rate of microwave heating in terms of electric

over

DD FORM 1 JAN 73 1473 EDITION OF 1 NOV 65 IS OBSOLETE

UNCLASSIFIED
SECURITY CLASSIFICATION OF THIS PAGE (When Data Entered)

H11 144

Block No. 20

ABSTRACT

field and material dependent parameters. The dielectric constant and loss tangent of gelled epoxy samples are measured and reported as functions of frequency and temperature. This information is used to develop a theoretical model for the microwave heating behavior of an epoxy during cure. The results of actual high power heating experiments are compared with the theoretical predictions. Physical mechanisms responsible for the observed behavior are proposed.

Best agreement between the theoretical model and the high power heating experiments is obtained by assuming that the curing epoxies exhibit a bulk loss tangent close to that of pure water, rather than the value measured for the gelled epoxy, and a dielectric constant approximately equal to that of the gelled material. This phenomena is attributed to hydroxyl groups both present in the uncured material and formed during cure. It is proposed that rapid microwave heating results due to energy absorption by these dipolar groups. Anomalies in the experimental heating data are attributed to the promotion of exothermic chemical reactions involved in the cure.

The observed dielectric properties of the epoxies suggest a depth of penetration sufficient for uniform cure of thick cross sections of epoxy. The rate of microwave heating is observed to be extremely rapid. It is concluded that the use of microwave heating to promote the cure of thick fiberglass/epoxy laminate structures is a viable alternative to conventional methods.

## FOREWARD

This project was accomplished as part of the U. S. Army Aviation Research and Development Command Manufacturing Technology program. The primary objective of this program is to develop, on a timely basis, manufacturing processes, techniques, and equipment for use in production of Army Material. Comments are solicited on the potential utilization of the information contained herein as applied to present and/or future production programs. Such comments should be sent to: U. S. Army Aviation Research and Development Command, ATTN: DRSAV-EXT, P. O. Box 209, St. Louis, MO 63166.

The work described in this report was funded by an Army Materials and Mechanics Research Center contract (DAAG46-76-C-0035) with Dr. Bernard M. Halpin, Jr. as the Contracting Officer's Technical Representative.

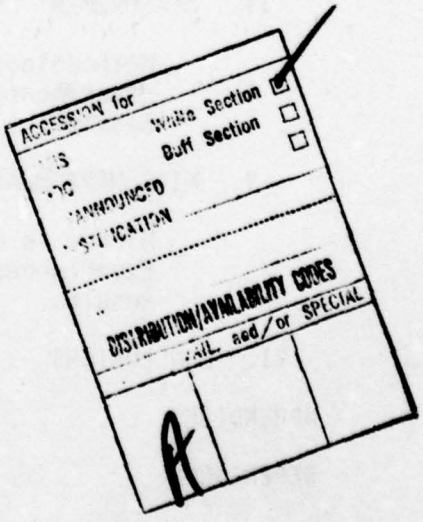




79 04 20 025

TABLE OF CONTENTS

## LIST OF FIGURES

# CHAPTER I

## INTRODUCTION

Fiberglass laminates have widespread application due to their superior chemical and mechanical properties. One form of these materials consists of alternating layers of epoxy and glass cloth. The combined properties of the epoxy binder and glass webbing result in a strong, lightweight structural material.

The fabrication process for these materials includes the hardening, or cure, of the liquid epoxy resin/curing agent system. The conventional curing technique involves promotion of a polymerizing chemical reaction by heating the laminate structure in a high temperature oven. However, this method results in a temperature gradient and non-uniform heating in thick sections of the material due to the low thermal conductivity of both the glass and epoxy. Under these conditions, the core of the structure may not always reach a sufficient temperature for complete cure of the epoxy. This effect can result in a weakened structure with properties unsuitable for its intended application.

The method of radio frequency heating may produce the desired uniform cure of thick fiberglass/epoxy laminates. The advantage of this technique is that heating occurs uniformly throughout a dielectric volume exposed to an appropriate time dependent electric field. However, an important consideration is that, in contrast to heating in a constant temperature environment, the temperature of the material increases

continuously during application of the electric field. Control of the radio frequency heating process is therefore required. Although the temperature of the dielectric can be measured during heating, the ability to predict the heating behavior based on an understanding of material and field dependent parameters is desirable for the process control.

It is proposed that radio frequency heating by microwave radiation is a viable solution to the problem of obtaining a uniform cure of the epoxies. In a similar application, microwave heating has been successfully employed by industry for the cure of urethane plastic [1]. Microwave heating has also been studied as it applies to the food industry [2,3,4] and application of this technique for drying wet materials has been investigated by the ceramics and lumber industries [5,6,7]. Preliminary investigations on the dielectric properties of epoxies by Salerno et al. [8] suggest microwave heating may be successfully employed for the processing of fiberglass/epoxy laminates.

The purpose of the work presented in this paper is to investigate the mechanisms responsible for the microwave heating behavior of epoxy systems during cure. This problem is approached by the formulation of a mathematical relation showing the dependence of microwave heating on the dielectric properties of a material and electric field parameters. The dielectric properties of the epoxies are then measured as functions of frequency and temperature. Using this information, a theoretical model predicting the microwave heating behavior of an epoxy during cure is developed. The results of actual high power heating experiments are compared with the theoretical predictions and physical mechanisms responsible for the observed behavior are proposed. The results of this

effort show microwave heating to be a viable alternative to conventional methods for curing fiberglass/epoxy laminates.

Chapters II and III present, respectively, summaries of epoxy chemistry and dielectric theory. Chapter IV describes the technique used in measuring the dielectric properties of the epoxies at microwave frequencies and presents the results of these measurements. The methods used in the high power heating experiments and an analysis of the results appear in Chapter V. The conclusions discussed in Chapter VI apply the results of this project to the cure of thick fiberglass/epoxy laminates by microwave heating.

# CHAPTER II

## STRUCTURE AND CHEMISTRY OF EPOXY

In order to understand the mechanisms involved in microwave heating of epoxies, it is essential to understand the basic chemistry of these materials. To that end, this chapter is a discussion of the general nature of epoxy resins, including their physical properties.

### Epoxy Resins

Epoxy resins, first synthesized in the late 1930's, are among the newest of the major industrial plastics. Epoxy resins are thermosetting materials meaning that, when converted by a curing agent, they form hard, infusible systems. The key to their physical properties is that the system formed is a three dimensional network in which the movement of a molecule in any direction is opposed by a crosslinking arrangement [9].

In contrast, thermoplastic resins, such as polyethylene and polyvinyl chloride, may be considered to be permanently fusible compounds. Their structures can be described as an assemblage of long, linear chains lying together in three dimensions but, under ordinary conditions, without three-dimensional crosslinking. The contrasting structures of thermosetting and thermoplastic resins are diagrammed, as viewed in a two-dimensional cross-section, in Figure 2-1. Note that the movement of a molecule in the thermoplastic resin is not restricted in all directions due to the lack of crosslinking with surrounding molecules.

The differences in structure between thermoplastic and thermosetting

resins, such as epoxies, effect the macroscopic properties of the materials.

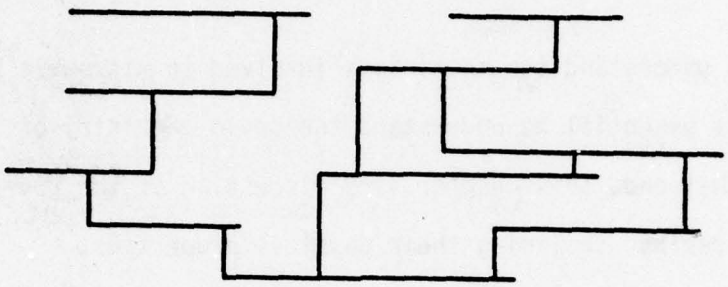

(a)

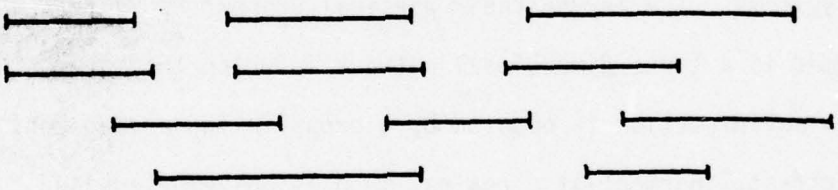

(b)

Figure 2-1: Two-dimensional diagrams illustrating the structure of (a) thermosetting and (b) thermoplastic materials.

Unlike thermosetting resins, which maintain their rigid dimensionality throughout their design range, thermoplastic materials will progressively soften when heated and flow with pressure. Note, however, that the design range for some thermosetting resins may be extremely limited,

with their properties rapidly deteriorating when these limits are exceeded. These and other differences, such as molding techniques, combine to make the class of thermosetting resins superior to thermoplastics in many industrial applications [9].

The properties of thermosetting epoxy resins that are most important in industrial applications are 1) versatility, 2) good hardening characteristics, 3) toughness, 4) high adhesive properties, 5) low shrinkage, and 6) inertness [9]. The versatility of epoxies is due to the availability of numerous curing agents and their compatibility with a wide variety of modifiers. Also, the ratio of the amount of curing agent to epoxy resin is not as critical as with some other thermosetting materials. This permits engineering for a wide diversity in the properties of the cured epoxy resin system. Cure can be accomplished in almost any specified time period by proper selection of a curing agent and regulation of cure cycles. The cure of epoxy resins differs from that of other thermosetting compounds in that no by-products result since cure is accomplished by direct addition of bridging molecules [9]. Shrinkage is usually on the order of 2 percent, indicating that little molecular rearrangement is necessary. Cure of other thermosetting materials involving condensation reactions result in significantly higher shrinkage. The resulting structure of cured epoxy resins, consisting of ether groups, benzene rings, and aliphatic hydroxyls, is chemically inert, being virtually invulnerable to caustic attack, extremely resistant to acids, and impervious to moisture.

## Structure and Characteristics of Epoxy Resins

The usable epoxy is a mixture of epoxy resin and curing agent. The structure and characteristics of epoxy resins will now be discussed. The details of cure by various curing agents will be considered later.

The characteristic feature of an epoxy resin molecule is the reactive epoxy group shown below:

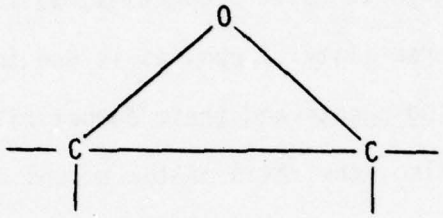

These groups serve as points of polymerization. Crosslinking and cure is accomplished through these or other groups resulting in a tough, extremely adhesive, and inert solid. The most common epoxy molecule of commerce is the diglycidyl ether of bisphenol A (DGEBA)

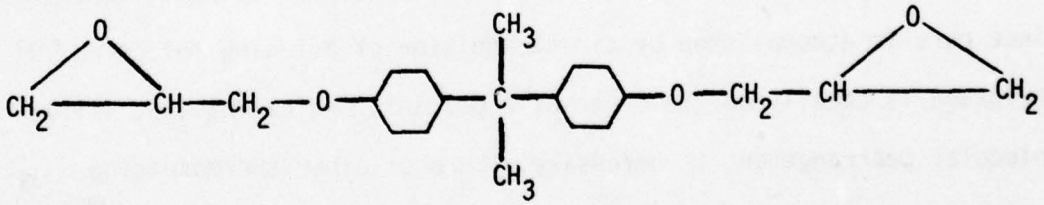

This structure is of particular interest because the epoxy resins examined in this research are either completely composed of this material (Epon 828) or are a mixture of this material and another resin (3M 1009) [10]. The synthesis of these compounds will not be discussed here but can be found in the literature [9,11]. Epoxy resins with higher molecular weights are also available. These molecules will, in general,

also contain no more than two epoxy groups. The general structure of an epoxy resin is represented as shown in Figure 2-2. Note that each molecule of the generalized epoxy contains the same number of alcoholic hydroxyls, n, as there are repeated groups.

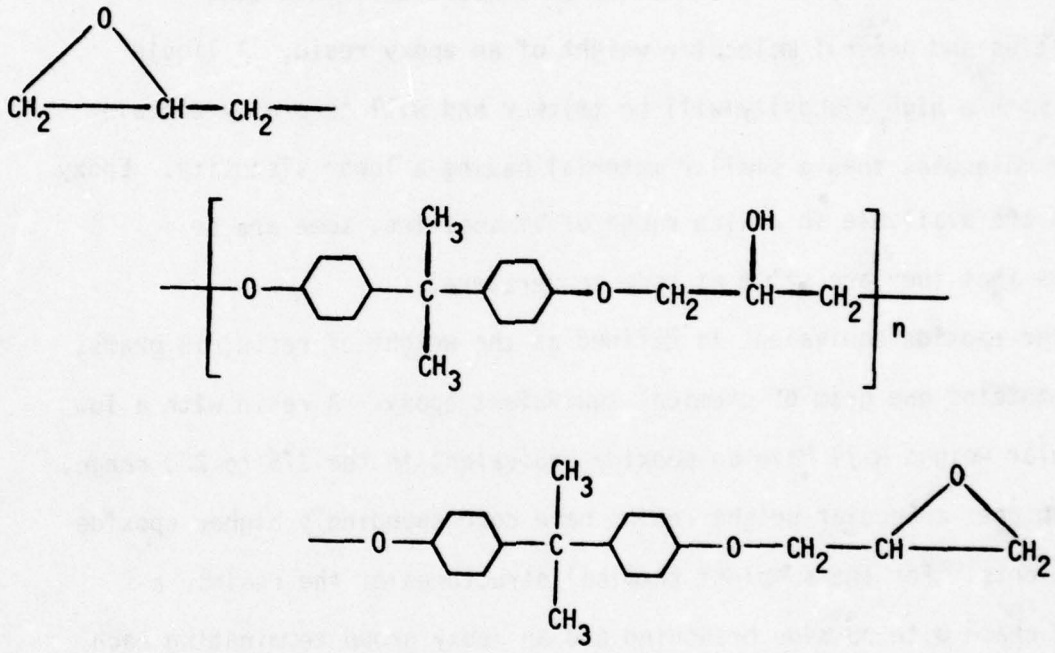

Figure 2-2: Generalized epoxy resin molecule.

Commercial epoxy resins are available for engineering applications with a wide range of properties. In order to determine if an epoxy is suitable for a particular application it is necessary to know the characteristics of that resin. There are six main characteristics of epoxy resins that serve as guides for predicting their structure and usefulness. These characteristics are viscosity, epoxide equivalent,

hydroxyl equivalent, average molecular weight and molecular weight distribution, softening point, and heat-distortion temperature [9]. These criteria will now be discussed.

The viscosity of a material is essentially a measure of its resistance to changing its form and can be considered a sort of internal friction. Therefore, it is useful as an indication of handling properties and general molecular weight of an epoxy resin. A liquid resin with a high viscosity will be thicker and will generally contain larger molecules than a similar material having a lower viscosity. Epoxy resins are available in a wide range of viscosities; some are so viscous that they are solid at room temperature.

The epoxide equivalent is defined as the weight of resin, in grams, that contains one gram of chemical equivalent epoxy. A resin with a low molecular weight will have an epoxide equivalent in the 175 to 200 range, while higher molecular weight resins have correspondingly higher epoxide equivalents. For the simplest chemical structures of the resins, a linear chain with no side branching and an epoxy group terminating each end, the epoxide equivalent is one half the average molecular weight of the resin. In addition to traditional titration methods, the epoxide equivalent can be determined by infrared spectroscopy. Prominent absorption bands in the infrared spectra of epoxy resins are at 2.95, 3.5, and 10.95μm and are attributed to hydroxyl, methylene, and epoxy groups, respectively. Epoxide equivalents are determined from the changes in band intensity that accompany the change in percentage of these various groups with different molecular weight resins.

Similar to the epoxide equivalent, the hydroxyl equivalent is the

weight of epoxy resin that contains one equivalent weight of hydroxyl groups. Infrared techniques are also suitable for hydroxyl equivalent determination. In contrast to the epoxide equivalent, the hydroxyl equivalent will generally, in simpler structures having a high degree of polymerization, remain constant as the molecular weight increases.

In commercial epoxy resins, the number of repeated units appearing in a molecule of resin varies considerably. Referring to Figure 2-2, the distribution of the percentage of molecules having different values of n will be weighted. For example, there may be a small percentage of molecules having n = 0 (monomers), a considerable number of polymers of n = 1 and n = 2, a larger percentage with n = 4 and n = 5, and a small percentage with n > 5. Due to the weighted distribution, the average molecular weight would indicate the resin to be entirely a polymer of n ≃ 4 or 5. However, the actual percentages of each polymer present are responsible for the structure and properties of the cured epoxy. Thus, it is important to know not only the average molecular weight of the resin, but also the percentage of each polymeric specie that contributes to the average molecular weight. This information is available through experimentation.

The softening point is defined as the temperature at which a resin reaches an arbitrary softness or viscosity. It is a method of qualitative evaluation of uncured resins and relates directly to the average molecular weight of the material, as indicated by Figure 2-3.

In contrast to all the previous characterization techniques, the heat-distortion test is employed in the evaluation of a cured resin system. The heat-distortion temperature is the temperature at which a

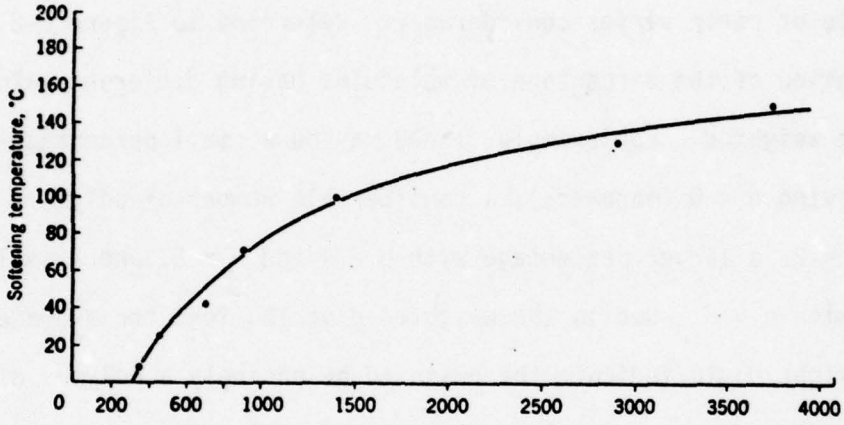


Figure 2-3: Resin softening point vs. molecular weight (after Lee and Neville [9]).

cured epoxy sample experiences a predetermined level of distortion while under a given mechanical load. This test is valuable in evaluating new resins or curing agents and in determining the proper amount of a curing agent to be used with a specific resin.

The number of epoxy resin types used commercially is relatively small compared to the number of possible epoxy resin molecules that can be synthesized. The epoxies studied in this research are resins based on DGEBA and an epoxylated novolac. The resin Epon 828 is a DGEBA type material manufactured by Shell Chemical Company and the resin 1009, manufactured by 3M Company, is a mixture of Epon 828 and a Dow Chemical Company epoxylated novalac, DEN 438. The general structure of a DGEBA-type resin has already been discussed. The corresponding structure of a general epoxylated novalac is represented as

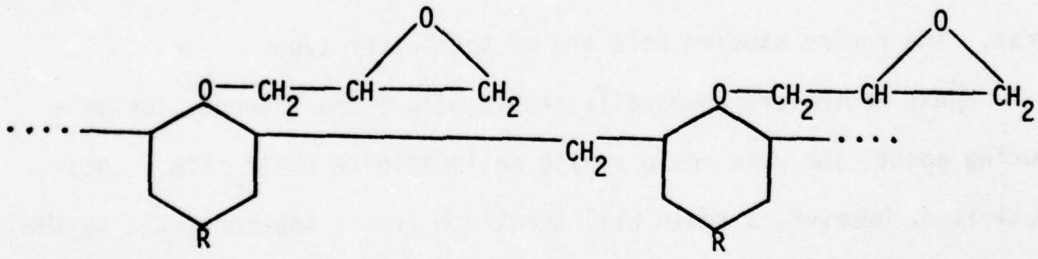

These resins generally result in higher heat distortion temperatures and better performance at high temperatures than do DGEBA-type epoxies.

As previously stated, the research work presented in this thesis was done using the Epon 828 and DEN 438 resins with specific curing agents. In the sections that follow, properties of epoxy resin and curing agent systems in addition to those studied will be given. This approach is necessary because of the limited literature available on the properties of specific interest. It is felt the discussion of the general nature

of the properties of interest will be sufficient to give the reader an appreciation of the data to be presented.

## Curing of Epoxy Resins

Epoxy resins are characterized by their ability to transform from a thermoplastic state to a hard, thermoset solid with the addition of a chemically active reagent called the curing agent. There are many reactions that can bring about the cure of an epoxy resin and, hence, there are many types of curing agents. While some curing agents participate directly in the reaction and become part of the polymerized chain, others merely promote polymerization through catalytic action. The mechanism for promotion of the reaction also depends on the particular agent used. The process may take place at room temperature, proceed with heat produced by exothermic reaction, or require external heat. The resins studied here are of the latter type.

Epoxy resins are chemically stable before the introduction of a curing agent, the pure resin having an indefinite shelf life. Once activated, however, a resin will transform from a thermoplastic to the thermoset state through at least one of the following reactions [9]:

1) direct linkage between epoxy groups,

2) linkage of epoxy groups with aromatic or aliphatic hydroxyls,

3) crosslinkage with the curing agent through various radicals.

These three processes will be considered separately in the discussion that follows.

Polymerization through epoxy groups takes place via a molecular linkage through the oxygen atom of an epoxy group. This linkage proceeds

by reaction of the epoxy resin with a tertiary amine ($R_3N$) curing agent. The tertiary amine reacts with the epoxy ring as follows:

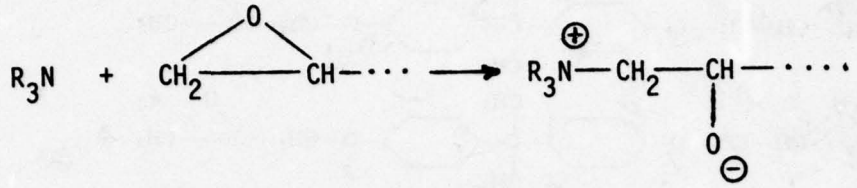

Thus the tertiary amine is capable of opening the epoxy ring. Assuming the polar nature of the resulting structure is capable of opening other rings, the reaction proceeds and results in the long chain structure:

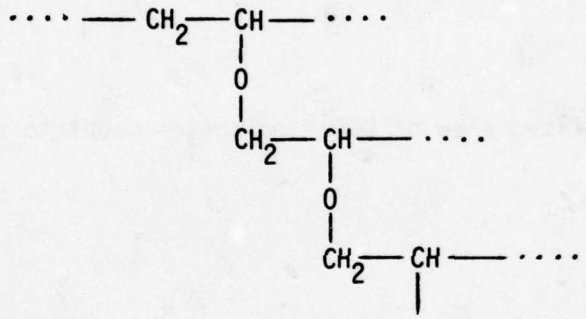

In order to visualize the final structure of the cured epoxy, consider several molecules of the monomer DGEBA lying side by side as shown in Figure 2-4. Under these idealized conditions, the reaction discussed above will result in the crosslinked polymerization of the epoxy resin to yield the structure shown in Figure 2-5. However, it is quite unlikely that the liquid resin molecules would ever line up uniformly as shown in Figure 2-4. Thus, the idealized two-dimensional structure of the cured epoxy will actually resemble that shown in Figure 2-6. Note that this is an idealized structure. The molecules actually arrange themselves in three dimensions to form a complex amorphous structure. The polymer chains are terminated by the blocking

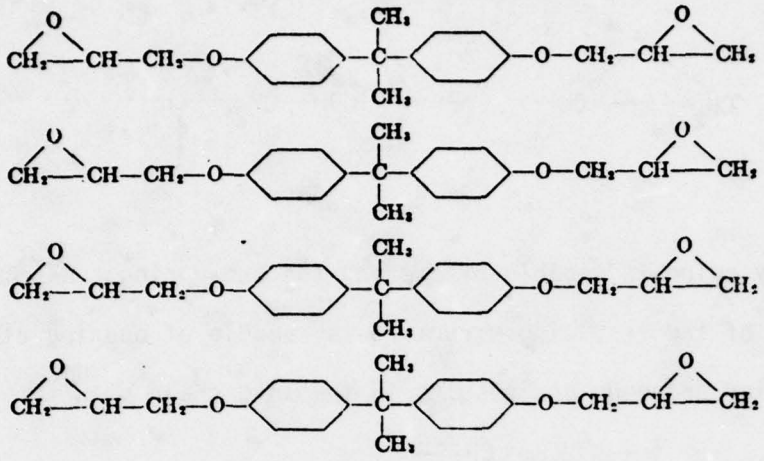

Figure 2-4: Idealized view of DGEBA molecules about to react.

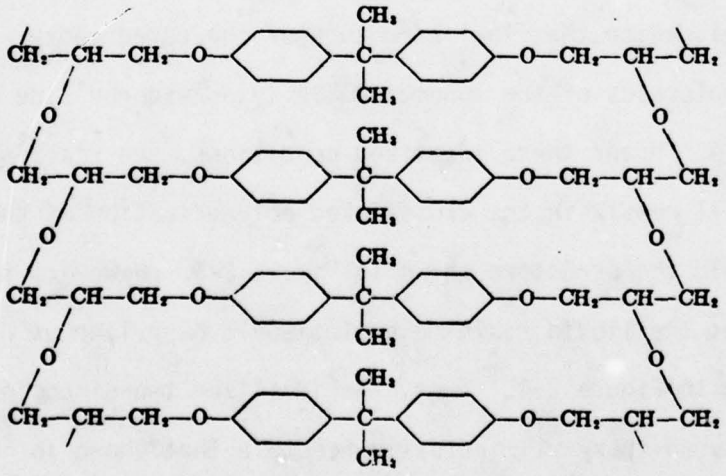

Figure 2-5: Idealized crosslinking of DGEBA molecules.

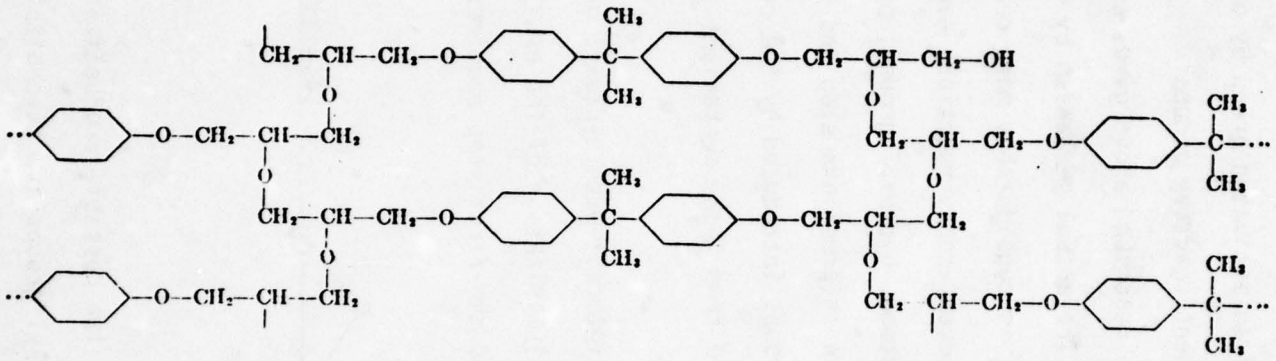

Figure 2-6: Idealized crosslinking of DGEBA molecules showing structure resulting from random molecular arrangement (after Lee and Neville [9]).

off or trapping of an activated group by other epoxy chains, leaving them without adjacent reactive groups.

The structure described above gives an accurate representation of the cured epoxy. The actual mechanism by which this structure is achieved, however, is considerably more complex. Polymerization rarely occurs via direct epoxy-epoxy reaction, even with a tertiary amine curing agent. Instead, hydroxyl groups, present in higher order polymer resins, enter as an intermediate step and crosslinking takes place through radical groups introduced by the curing agent. However, the structure resulting from these mechanisms is best described by the above representation.

Epoxy groups interact with hydroxyl groups as an intermediate step to crosslinking polymerization of the epoxy resin. These groups do not interact easily and the first step requires activation by a catalyst:

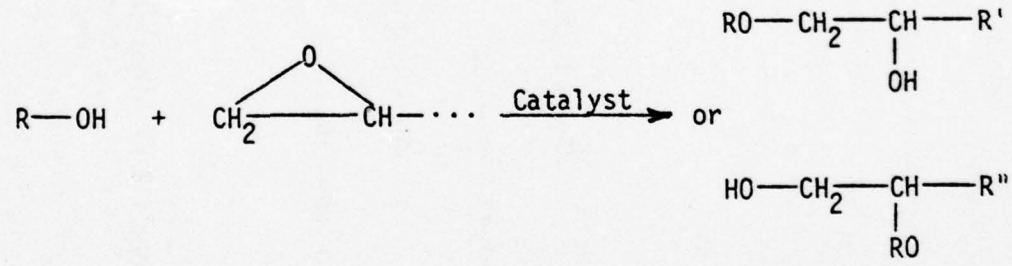


Although there are two possible products of this first reaction, both of these new hydroxyl groups are susceptible to continued polymerization. For example, the process may proceed as

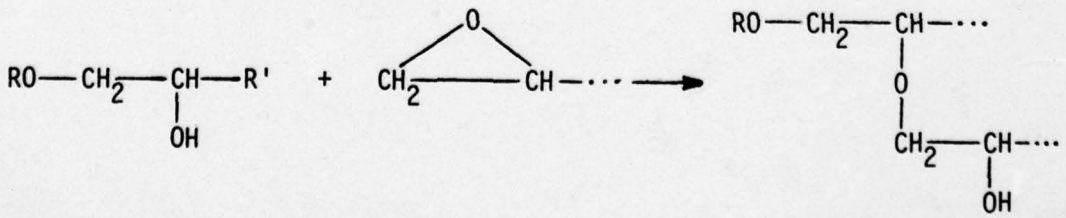

This structure is very similar to that resulting from the direct epoxy-epoxy polymerization discussed previously. This reaction, once catalyzed, proceeds very rapidly and can continue until a high degree of crosslinking is achieved.

The principle agents used in promoting resin cure by epoxy-hydroxyl reactions are tertiary amines. This catalyst opens the epoxide ring, as discussed previously, permitting polymerization through hydroxyls to occur. An important aspect of this type of polymerization is the appearance of hydroxyl groups during intermediate reactions. This will be considered again in the discussion of microwave heating mechanisms in the resin-curing agent system.

The method of curing by a crosslinking agent refers to the use of a reactive intermediate to join the resin chains [9]. The principle crosslinking agents used to cure epoxy resins are primary ($RNH_2$) and secondary ($R_2NH$) amines and acid anhydrides. In order to study the basic mechanism for cure by crosslinking agents, consider the sequence of reactions that occur with primary amines. The first step is a reaction with an epoxy group to form a secondary amine

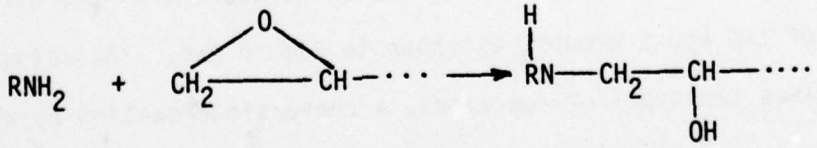

Next is a reaction with another epoxy group to form a tertiary amine

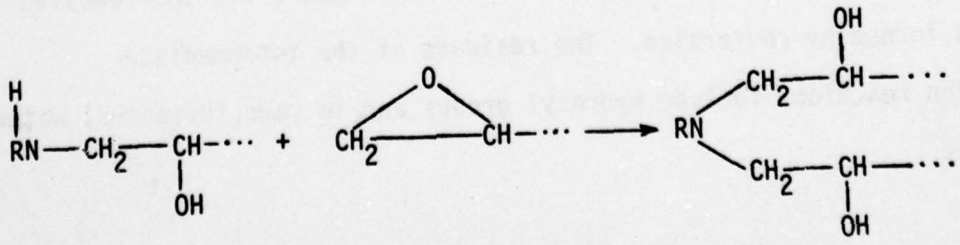

The final step is the reaction of these intermediate hydroxyls with another epoxy group

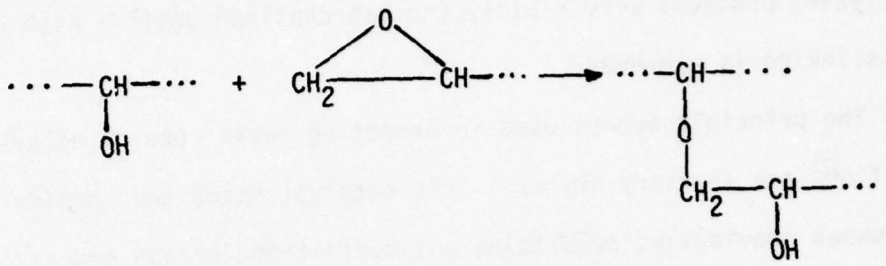

resulting in crosslinking polymerization of the resin. The resulting structure of the cured epoxy is the same as that proposed earlier for direct epoxy-epoxy polymerization. Also, note the formation of hydroxyl groups during the intermediate reactions. Again, these will be considered in the discussion of mechanisms for microwave heating. As previously mentioned, acid anhydrides also promote a similar series of reactions; hydroxyl groups and water are intermediate by-products.

In summary, the primary mechanisms responsible for crosslinking polymerization of epoxy resins are linkage of the epoxy groups through hydroxyls and linkage via a reactive intermediate agent. Both of these mechanisms result in a structure that can be represented by the direct interaction of two epoxy groups, as shown in Figure 2-6. The actual process involves two types of reactions, a conversion reaction by which the reactive agents are broken down and a crosslinking reaction in which molecules are coupled into a three-dimensional network via the reactive residues formed by conversion. The residues of the intermediate conversion reactions include hydroxyl groups and, in some instances, water molecules.

## Characterization of Cured Epoxy Resins

The degree of cure of an epoxy resin refers to the extent to which epoxy groups and the reactive species in the curing agent have been consumed. In practice, a system is considered thoroughly cured when the degree of crosslinking is such that the epoxy exhibits the optimum physical properties required for the particular application. The degree of cure achieved depends on the amount of curing agent used and the time and temperature of the cure cycle. Due to the complexity of the reactions involved, a theoretical model for determining the optimum cure cycle for a given system has never been formulated [9]. Some epoxy systems require application of external heat to promote curing while others, once activated, proceed with heat generated by exothermic reaction. Generally, proper cure cycles are determined empirically for each application.

The degree of cure can be determined in the laboratory by infrared spectroscopy or by chemical analysis. The results of the infrared spectroscopy method are of particular interest. The spectra of an epoxy resin cured with a primary aliphatic amine and a tertiary aliphatic amine are shown in Figures 2-7 and 2-8, respectively, as a function of curing time. The absorption bands of interest occur at wavelengths of approximately 3.0, 9.0 and 10.95μm and are attributed to hydroxyl groups, ethers, and epoxy groups, respectively. This data shows the increase in the number of hydroxyl groups and ether bonds, and the corresponding decrease in epoxy groups, as the degree of cure increases. This data will be referred to again in the discussion of possible microwave heating mechanisms in epoxies during cure.

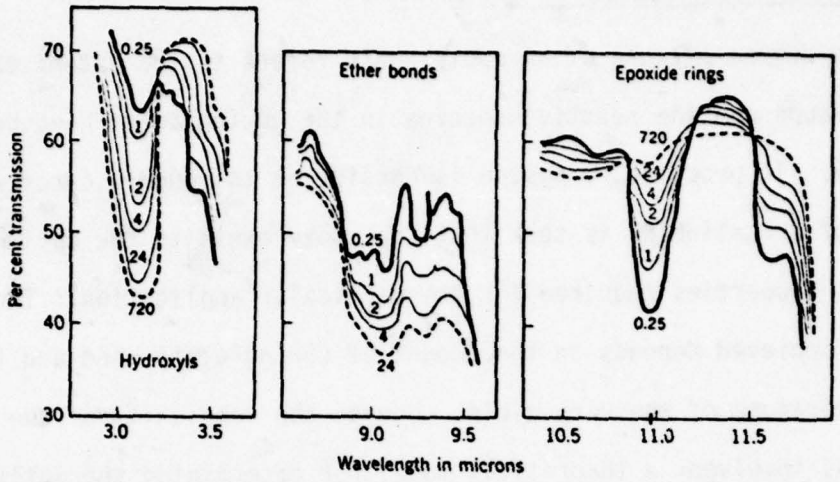


Figure 2-7: Infrared spectra of epoxy resin during cure with primary aliphatic amine. Numbers indicate cure time at 23°C (after Lee and Neville [9]).

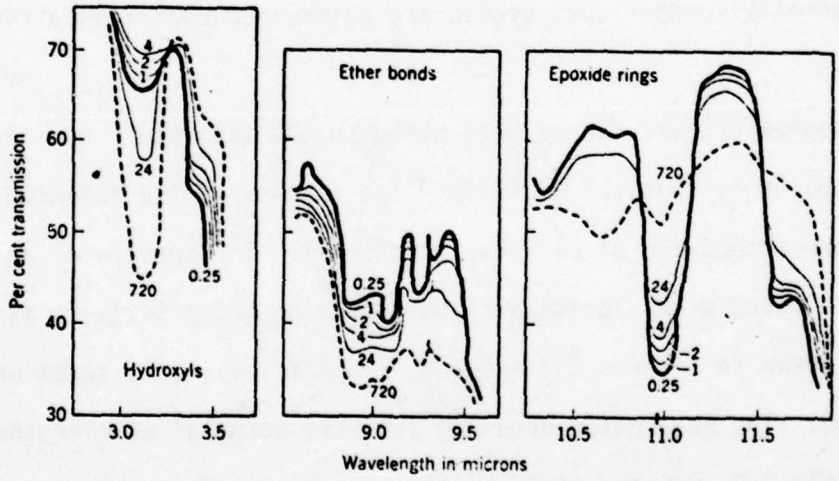


Figure 2-8: Infrared spectra of epoxy resin during cure with tertiary aliphatic amine. Numbers indicate cure time at 23°C (after Lee and Neville [9]).

Infrared techniques yield information concerning the degree of conversion of the species involved. The degree of crosslinking is also an important consideration in evaluating degree of cure. Measurement of crosslinking is done indirectly by determining heat-distortion temperature and solvent resistance.

A cured epoxy resin may be characterized by its physical, chemical and electrical properties. The physical properties considered in the characterization are heat-distortion, strength, impact resistance, hardness and flammability. Chemical properties are determined by exposing the epoxy to a chemically reactive atmosphere and measuring the effect of this exposure on the physical properties of the sample. Electrical properties considered in characterization are usually the dielectric constant, electrical loss, resistivity, dielectric strength, and arc resistance. Note that the electrical properties of cured resins are not of primary interest in this research. The topic of concern is the way in which the electrical properties change during cure. It should also be noted that the properties of a cured epoxy will depend critically on the type and amount of curing agent used. The cured system will probably not be at optimum in all its properties but will be a compromise to achieve the best overall performance in a specific application.

## Specific Epoxy Systems of Interest

The epoxy resins studied in this research are Epon 828, manufactured by Shell Chemical Corporation, and 3M Corporation's 1009. Epon 828 is a diglycidyl ether of bisphenol A and 3M 1009 is a resin system based on a 2 to 1 mixture of a Dow Chemical epoxy novalac, DEN 438, and Epon 828 [10].

Figure 2-9 shows the chemical structure and I.R. spectra for absolute DGEBA, Epon 828, and DEN 438. The curing agents studied are T-403, manufactured by the Jefferson Chemical Company, Z, nadic methyl anhydride (NMA), and boron trifluoride adduct with monoethylamine ($BF_3$-MEA). Benzyl dimethylamine (BDMA) is used as a reaction accelerator. These agents were used to form four epoxy systems, mixed as follows:

1) 100 part of 828 to 49 parts of T-403
2) 100 parts of 828 to 20 parts of Z
3) 100 parts of 828 to 90 parts of NMA with 2 parts of BDMA
4) 100 parts of 1009 to 3 parts of $BF_3$-MEA.

All materials were supplied by the Army Mechanics and Materials Research Center (AMMRC).

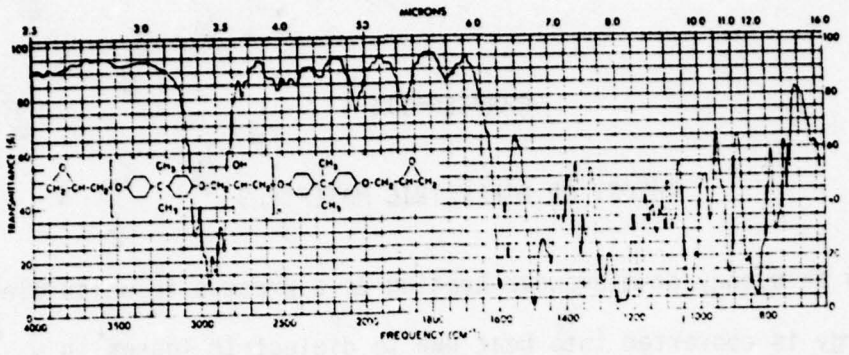


(a)

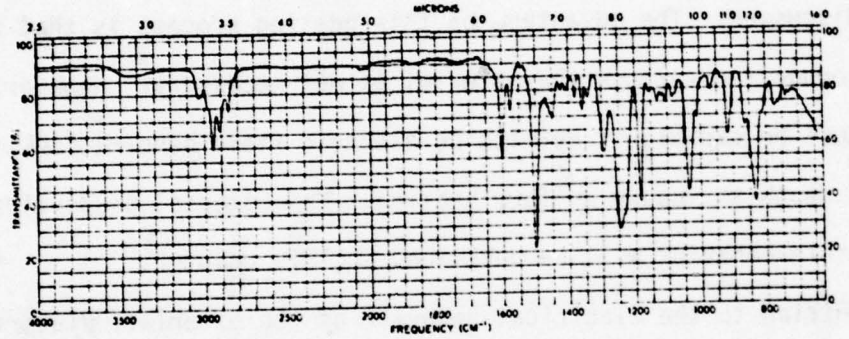


(b)

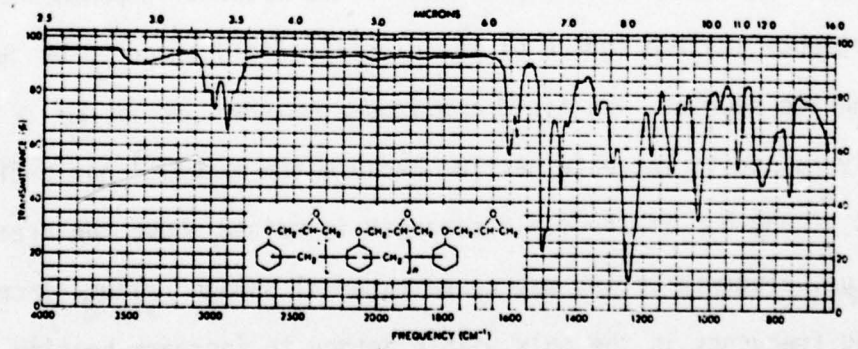


(c)

Figure 2-9: Infrared spectra of (a) diglycidyl ether of bisphenol A (n=0); (b) standard commercial DGEBA resin (n=0.2) EPON 828; and (c) epoxylated novalac DEN 438 (after Lee and Neville [11]).

# CHAPTER III

## THEORY OF DIELECTRIC MATERIALS

Radio frequency or microwave heating is a process in which electric field energy is converted into heat due to dielectric losses in a material [12]. The wide range of industrial application of this process has been discussed. The advantage of this heating process is that thermal heat conduction through the material is not necessary. However, the material must be capable of permitting electric field penetration to a sufficient depth to insure uniform heating. The material properties governing this behavior will be described in this chapter.

In addition to the electrical behavior of the material, electric field frequency and strength are important heating parameters. It will be seen that the amount of heat produced in the material depends directly on the frequency and the square of the electric field produced by the electromagnetic source. The field amplitude, however, cannot be arbitrarily raised to increase heating because the material has a finite dielectric strength. If the field strength is raised above the breakdown voltage, electric arcing may cause material damage. Thus, increasing the working frequency is the only usable method to increase heating of a given material. This reason, together with the decrease in depth of penetration at higher frequencies, results in the microwave frequency region being optimal for electric field heating.

The purpose of this chapter is to develop a quantitative expression

describing the heating of a dielectric in an electromagnetic field. The expression developed is to contain only parameters that are measurable by experiment. In order to understand the heating process, however, it is necessary to consider the action of an electric field on a dielectric at a molecular level. The parameters of interest may then be related to macroscopically observable quantites and developed into a general relation.

This chapter will proceed by describing the interaction of electromagnetic energy with dielectric media, relating macroscopically observable quantities to molecular parameters, considering the nature of these important variables, and finally, deriving an equation relating heating rate to measurable parameters. The electrical parameters involved are dielectric constant, loss tangent, frequency, and field strength. The dielectric constant and loss tangent, being material dependent, will be discussed at length.

## Interaction of an Electric Field with a Dielectric

An ideal dielectric material, being perfectly non-conducting, interacts with an electric field through displacement of its charge carriers from their equilibrium positions. This behavior can be studied by considering a time independent electric field acting on the dielectric of a parallel plate capacitor. The magnitude of the force acting on a carrier of charge e is

$$F = eE = e\frac{V}{d},$$

where V is the voltage across the capacitor and d is the plate separation.

The phenomena of polarization results in the formation of positive and negative charges at opposite surfaces of the dielectric in response to this force. This can be pictured (Figure 3-1) as the formation of dipole chains aligned parallel to the applied field and binding countercharges at the electrodes. The density of this neutralized surface charge is called the polarization of the dielectric.

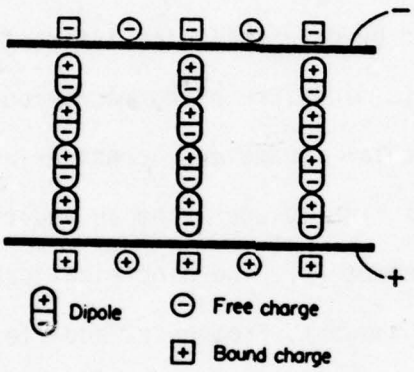


Figure 3-1: Schematic representation of dielectric polarization.

For a capacitance $C_o$, the charge on the capacitor plate is

$$Q = C_o V.$$

The "relative dielectric constant" $\varepsilon_R'$ is an independent parameter associated with the material and is given as the quotient of the material permittivity, $\varepsilon'$, and the permittivity of free space, $\varepsilon_o$. Accordingly,

$$\varepsilon_R' = \varepsilon'/\varepsilon_o.$$

The number of charge carriers neutralized through polarization at the interface of the dielectric and electrode is [12]

$$Q(1 - 1/\varepsilon_R').$$

Therefore the number of free charge carriers that remain at the interface is

$$\frac{Q}{\varepsilon_R'} .$$

These free charges constitute the source of the electric field acting on the polarized dielectric. Thus, it can be regarded that the applied electric field $\vec{E}$ is opposed by a "polarization field" $\vec{P}$ resulting in the polarized dielectric experiencing a field $\vec{D}$ called the "displacement field." This field is given as

$$\vec{D} = \varepsilon'\vec{E} = \varepsilon_o\varepsilon_R' \vec{E},$$

with

$$\vec{D}_{FS} = \varepsilon_o\vec{E}$$

in free space where $\varepsilon_R' = 1$. Therefore the polarization can be expressed as the difference between the displacement field in the material and in free space

$$\vec{P} = \vec{D} - \vec{D}_{FS} = \vec{D} - \varepsilon_o\vec{E}$$

or,

$$\vec{P} = (\varepsilon_R' - 1)\varepsilon_o\vec{E}[\frac{coul}{m^2}] . \qquad \text{(III-1)}$$

The "dielectric susceptibility"

$$\chi = \varepsilon_R' - 1,$$

gives the ratio of neutralized to free charge carriers.

In addition to being a measure of neutralized surface charge density, the magnitude of the polarization vector is also equivalent to the dipole moment per unit volume of the dielectric. This latter interpretation permits a development of macroscopic process via an analysis at the molecular level [12]. This development will now be considered.

The dipole moment per unit volume can be considered the result of the additive action of N elementary dipole moments $\vec{\mu}$. Thus,

$$\vec{P} = N\vec{\mu}. \qquad \text{(III-2)}$$

These dipole moments occur as the reaction of elementary particles, or "polarization sites," to the local electric field $\vec{E}'$ acting in the vicinity of these sites. It may be assumed that the magnitude of the dipole moment is proportional to the local field strength

$$\vec{\mu} = \alpha\vec{E}'. \qquad \text{(III-3)}$$

The constant of proportionality $\alpha$ is called the "polarizability" and has dimensions

$$[\alpha] = [\frac{s^2 coul^2}{kg}] = [\varepsilon m^3]$$

in the mks system. As the ratio of dipole moment to local field strength, $\alpha$ is essentially a measure of the electrical pliability of the polarization site [13].

Combining equations (III-1), (III-2), and (III-3)

$$\vec{P} = (\varepsilon_R' - 1)\varepsilon_o\vec{E} = N\alpha\vec{E}' \qquad \text{(III-4)}$$

Thus the macroscopically observable permittivity is related to three molecular parameters: the number N of contributing polarization sites, their polarizability $\alpha$, and the local electric field $\vec{E}'$ acting at the sites. The local field $\vec{E}'$ will normally differ from the externally applied field $\vec{E}$ due to polarization of the surrounding medium, as will be discussed later. The goal of this chapter is to understand the dependence of these parameters on frequency, temperature, and applied field strength in order to understand the mechanism of microwave heating.

There are four types of molecular level polarization that lead to macroscopically observed effects [13]. These four types of polarization arise from the same basic condition that matter consists of positively charged atomic nuclei surrounded by a negative electron cloud.

When influenced by an external electric field, an atom's electrons are displaced slightly with respect to the nucleus. The result is "induced" dipole moments and "electronic polarization" of materials. The combination of different types of atoms to form molecules usually results in an asymmetric distribution of electrons around the nuclei and the formation of net charge sites of opposite polarity. The displacement of these charge sites from their equilibrium positions by an external field leads to a second type of induced dipole moment and "atomic polarization." In addition, this net charge distribution results in permanent dipole moments that exist even in the absence of an external field. The tendency of these dipoles to align themselves in the direction of an applied field gives rise to "dipole polarization". The fourth type of polarization occurs due to the motion of free charge carriers through an imperfect dielectric subject to an external field. The trapping of

these charges in the material, at interfaces, or at electrodes results in a space charge distribution and macroscopic field distortion. Resulting in an increase in capacitance and, hence, permittivity, this behavior is called "space charge polarization".

The first three types of polarization discussed above are due to locally bound charge while the latter is due to charges that can migrate for some distance through the dielectric. These polarization mechanisms are characterized by an electronic polarizability $\alpha_e$, an atomic polarizability $\alpha_a$, a dipole polarizability $\alpha_d$, and a space charge polarizability $\alpha_s$. Assuming the four polarization mechanisms are independent of each other [13], the total polarizability of a dielectric may be written

$$\alpha = \alpha_e + \alpha_s + \alpha_d + \alpha_s.$$

These four effects determine the response of a dielectric to an applied field.

As seen from equation (III-4), the behavior of the permittivity depends on the parameters N, $\alpha$, and $\vec{E}'$. Primary dependence, however, is on the polarizability $\alpha$ [13]. Therefore, the approach shall be to express the dielectric constant in terms of $\alpha$, eliminating N and $\vec{E}'$ by approximation.

In solids and liquids, the local field $\vec{E}'$ acting at a polarization site will differ from the external field $\vec{E}$ due to polarization of the surrounding material. Consider the dielectric of a parallel plate capacitor as shown in Figure 3-2. Imagine a reference molecule A surrounded by a sphere such that the polarization is constant outside

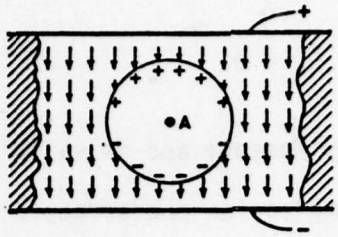


Figure 3-2: Model of dielectric structure for calculation of internal field $\vec{E}'$.

this sphere. The total field acting on A has three components: a field $\vec{E}_1$ produced by free charges at the electrodes, a field $\vec{E}_2$ produced by the charged ends of the dipole chains at the sphere's surface, and a field $\vec{E}_3$ produced by neighboring dipole polarization sites inside the sphere. Thus

$$\vec{E}' = \vec{E}_1 + \vec{E}_2 + \vec{E}_3.$$

The field $\vec{E}_1$ is, by definition, equal to the applied field $\vec{E}$,

$$\vec{E}_1 = \vec{E}.$$

The field $\vec{E}_2$ is calculated to be [13]

$$\vec{E}_2 = \frac{1}{3\varepsilon_o}\vec{P} = \frac{\vec{E}}{3}(\varepsilon_R' - 1).$$

Evaluation of the field $\vec{E}_3$ would require knowledge of the geometrical arrangement and polarizability of the molecular polarization sites inside the sphere. It is reasonable to assume, in certain cases, that the individual fields of the molecules surrounding A mutually cancel and

$$\vec{E}_3 = 0.$$

This assumption was first made by Mossoti and is valid for a number of cases, one of which is when the molecules are arranged with complete disorder, as is nearly the case for the epoxy resins [13].

Thus the local field acting at a polarization site is

$$\vec{E}' = \vec{E}_1 + \vec{E}_2 = \vec{E} + \frac{\vec{P}}{3\varepsilon_o} = \frac{\vec{E}}{3}(\varepsilon_R' + 2),$$

expressed in macroscopically observable parameters. Combining previous equations,

$$\vec{P} = (\varepsilon_R' - 1)\varepsilon_o\vec{E} = N\alpha\vec{E}' = \frac{N\alpha\vec{E}}{3}(\varepsilon_R' + 2)$$

implying that

$$\frac{N\alpha}{3\varepsilon_o} = \frac{(\varepsilon_R' - 1)}{(\varepsilon_R' + 2)}. \qquad \text{(III-5)}$$

The local field has been eliminated from the expression for permittivity. The value of N is now of concern. For an ideal gas at STP, N equals the "Loschmidt number" [13]

$$N_L = 2.687 \times 10^{25}\ [m^{-3}].$$

In the case of condensed matter, it is useful to evaluate N by considering the "molar polarization." The number N is related to the number of molecules per mole by

$$N = \frac{N_A\rho}{M},$$

where $N_A$ is Avogadro's Number, M is the molecular weight in [kg], and $\rho$ is the density in [kg $m^{-3}$], in the mks system. Substitution into equation (III-5) gives the "Clausius-Mosotti" equation

$$\Pi = \frac{N_A \alpha}{3\varepsilon_o} = \frac{\varepsilon_R' - 1}{\varepsilon_R' + 2} \frac{M}{\rho} \quad [m^3] \qquad \text{(III-6)}$$

where $\Pi$ is called the molar polarization. This is a key equation in that it relates the unknown molecular parameter $\alpha$ to macroscopically observable parameters.

Effects in a Time Dependent Field

The reactions of a dielectric to an applied electric field as discussed previously describe the effects which occur in a steady state field. In this section, the effects of time dependent field variations are considered. When a time independent field is applied, the polarization behaves as shown in Figure 3-3.

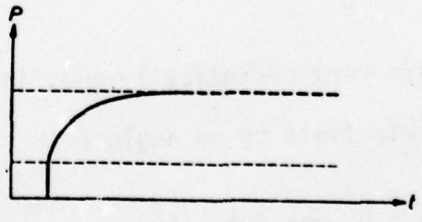


Figure 3-3: Dielectric polarization in a static electric field.

Observe that a pure elastic polarization takes place immediately for some types of polarization sites while the remainder require a finite time for alignment. This behavior, suggesting internal friction mechanisms resisting changes in dipole orientation, is also shown in Figure 3-4 where the field is applied at time $t_1$ and turned off at $t_2$. Note the immediate response of the elastic polarization sites at $t_2$ and the finite relaxation time required for other dipoles.

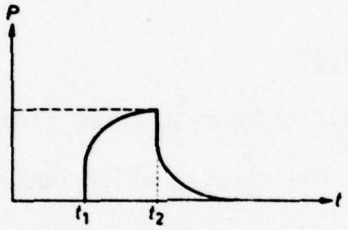


Figure 3-4: Dielectric polarization in a time dependent field.

Consider a dielectric experiencing an alternating electric field

$$\vec{E} = E_o \cos \omega t.$$

The displacement field will also vary periodically and, in general, will be out of phase with the electric field by an angle $\delta$

$$\begin{aligned} \vec{D} &= D_o \cos (\omega t - \delta) \\ &= D_o \cos \delta \cos \omega t + D_o \sin \delta \sin \omega t \\ &= D_1 \cos \omega t + D_2 \sin \omega t. \end{aligned}$$

The amplitudes $D_1$ and $D_2$ can be related to the amplitude $E_o$ by two

frequency dependent dielectric constants

$$D_1 = \varepsilon'(\omega)E_o$$
$$D_2 = \varepsilon''(\omega)E_o.$$

The "loss tangent" of the dielectric is defined as[†]

$$\tan\delta = \frac{D_2}{D_1} = \frac{\varepsilon''}{\varepsilon'}$$

and the "complex permittivity" is defined as

$$\varepsilon^* = \varepsilon_o\varepsilon_R^* = \varepsilon_o(\varepsilon_R' - j\varepsilon_R'').$$

Thus the displacement vector can be written

$$\vec{D} = \varepsilon^*\vec{E} = \varepsilon_o(\varepsilon_R' - j\varepsilon_R'')\vec{E},$$

indicating two components 90 degrees out of phase. The complex permittivity is therefore derived from the phase difference between the displacement and electric vectors for an applied time dependent electric field.

With the introduction of complex permittivity, the previously derived equations must be modified. For example, equations (III-5) and (III-6) become

$$\frac{N\alpha}{3\varepsilon_o} = \frac{(\varepsilon_R^* - 1)}{(\varepsilon_R^* + 2)} \qquad \text{(III-7)}$$

---

[†]Dielectric loss is actually proportional to $\sin\delta$. The use of $\tan\delta$ as a loss indicator is accurate only for small $\delta$ such that $\tan\delta \simeq \sin\delta$.

and

$$\Pi = \frac{N_A \alpha}{3\varepsilon_o} = \frac{\varepsilon_R^* - 1}{\varepsilon_R^* + 2} \frac{M}{\rho} , \qquad \text{(III-8)}$$

where $\alpha$ is now a complex quantity.

The frequency dependence of the complex permittivity, illustrated in Figure 3-5, is best understood by considering the different types of polarizability. In the case of electronic polarization, the external field deflects electrons from their original path inducing a dipole moment

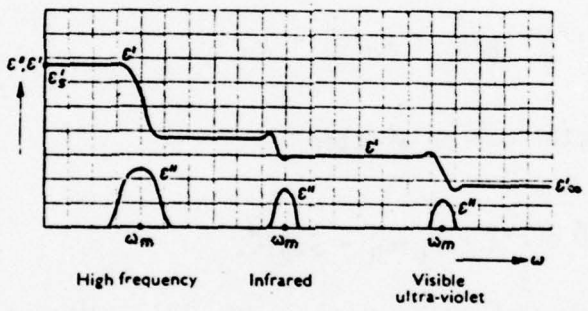


Figure 3-5: Frequency dependence of complex permittivity.

opposite to the applied field. The magnitude of this induced moment is proportional to the applied field strength but, with resonance in the visible or ultra-violet regions, is independent of the microwave frequencies. The extremely short relaxation time of these dipoles, compared to microwave radiation periods, results in an extremely small phase difference between the displacement and electric fields, and hence, virtually no dielectric losses.

Observed in materials where molecular groups have two different atoms bonded together, atomic polarization also results from induced

dipole moments. This phenomenon occurs when molecules are formed by atoms of different charge, such as ionic compounds, or when the bonding results in asymmetric electron distribution. Application of the electric field causes the charge centers to be displaced from their equilibrium positions, stretching or contracting the bond length, in proportion to the field strength. The resonant frequency for atomic polarization is in the infrared and, as with electronic polarization, contributes very little to microwave frequency losses.

In contrast to electronic and atomic polarization, dipole polarization has its resonance in the microwave region. This type of polarization occurs in materials whose molecules are natural dipoles, usually as a result of the asymmetric charge distribution associated with covalently bonded unlike atoms. Usually, an external field causes rotation of the dipole until it is aligned in the direction of the field. These dipoles respond to microwave frequencies in such a way that there is a phase shift between the displacement and electric vectors and, hence, electrical losses. This loss mechanism, which can be viewed as due to internal friction resisting the dipole rotation, is responsible for microwave heating of dielectric materials. Thus dipole polarization is the mechanism for microwave heating.

The effects of polarization on the complex permittivity were shown in Figure 3-5. Being of primary interest, the complex permittivity of dipolar molecules is discussed in the next section. Before continuing, however, recall that a decrease in $\varepsilon_R'$ implies a decrease in the ratio of neutralized to free charge carriers. Thus the behavior of the dielectric constant (Figure 3-5) shows that increasing frequency beyond resonance

decreases the number of polarized sites available to counter the free charges.

Dielectric Properties of Dipole Molecules

The previous section has shown that the behavior of a dielectric in an alternating electric field is governed by the dynamic properties of its atoms and molecules. Therefore, the dielectric behavior is more complicated in an alternating field than in a static applied field. Due to the phase difference between the electric and displacement field it is necessary to introduce a complex permittivity, its real and imaginary parts being denoted by $\varepsilon_R'$ and $\varepsilon_R''$, respectively. The behavior of these parameters as a function of temperature and frequency is the subject of this section.

Concerned with the effects of microwave frequency fields, the influence of the electric field on polar molecules, which exhibit a natural moment, is of interest. Consider the polar molecule $NH_3$ shown in Figure 3-6. This molecule has two equilibrium states, A and B, separated by an activation energy, $E_A$. In the absence of an electric field, the molecule is in thermal equilibrium and there is equal probability of transition to either state. For instance, thermal fluctuations can supply sufficient energy for a molecule in the A state to overcome the potential barrier and make the transition to the B state. Application of an electric field changes the probability of transition between these equilibrium states. This redistribution of equilibrium states results in the effective rotation of dipolar molecules in an alternating field and leads to dipole polarization of the dielectric.

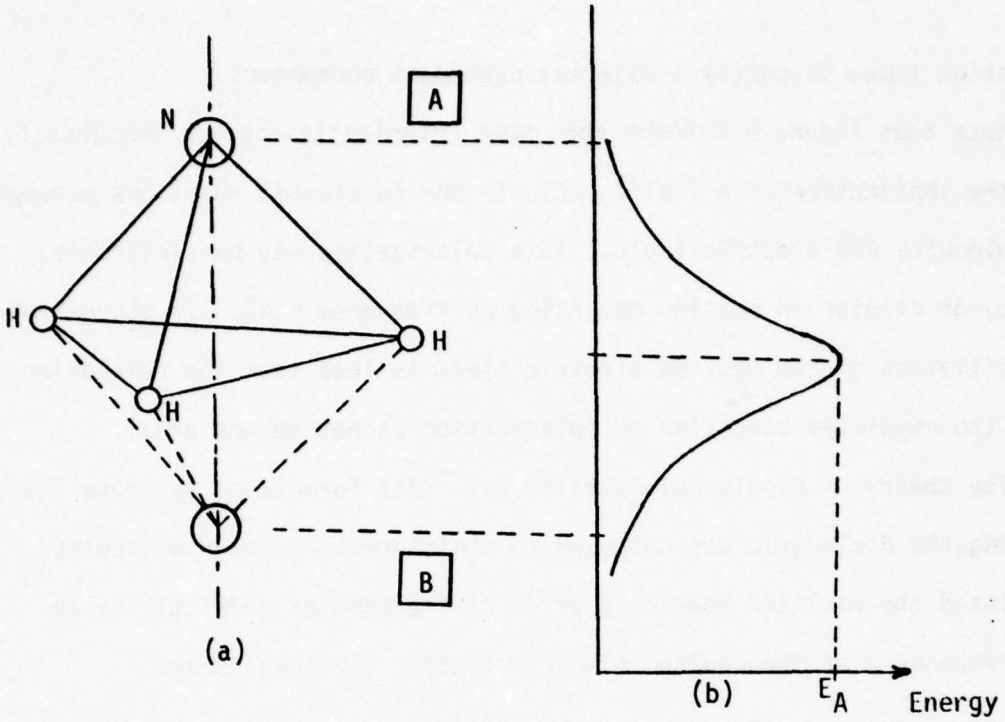


Figure 3-6: Dipolar $NH_3$ molecule showing (a) two equilibrium positions and (b) energy configuration.

The relaxation time apparent in Figure 3-4 shows that the dipole needs time to go from the state of random thermal agitation to the regulated condition of polarization. This relaxation time, $\tau_m$, can be expressed through the polarizability,

$$\alpha \propto e^{-(t/\tau_m)}.$$

Associated with the relaxation time is a natural frequency $\omega_m$, for transition between unpolarized and polarized states,

$$\omega_m = \frac{1}{\tau_m},$$

The natural frequency represents a resonance condition and, like the

relaxation time, is purely a material dependent parameter.

Note that Figure 3-4 shows that some polarization occurs immediately with the application of a field. This is due to elastic reactions between the molecules and electric field. This polarization may be electronic, atomic, or dipolar in origin, depending on frequency [14]. If the period of oscillation of the applied electric field is less than the relaxation time, the regulated condition of polarization cannot be achieved.

The theory of dipole polarization was first formulated by Debye [15]. Assuming the dielectric was composed of noninteracting polar molecules, he related the real and imaginary parts of the complex permittivity to the frequency $\omega$ of the applied electric field. The results are

$$\varepsilon_R'(\omega) = \varepsilon_\infty' + \frac{\varepsilon_s' - \varepsilon_\infty}{1+\omega^2\tau_m^2} \qquad \text{(III-9)}$$

$$\varepsilon_R''(\omega) = \frac{(\varepsilon_s'-\varepsilon_\infty')\omega\tau_m}{1+\omega^2\tau_m^2} \qquad \text{(III-10)}$$

$$\tan\delta = \frac{\varepsilon_R''(\omega)}{\varepsilon_R'(\omega)} = \frac{(\varepsilon_s'-\varepsilon')\omega t_m}{\varepsilon_s' + \varepsilon_\infty'\omega^2\tau_m^2} \qquad \text{(III-11)}$$

where $\varepsilon_\infty'$ and $\varepsilon_s'$ are the values of the relative dielectric constant for optical, $\omega\to\infty$, and static, $\omega = 0$, conditions, respectively. The behavior of the complex permittivity in the microwave region is shown in Figure 3-7. The loss, expressed as tan $\delta$, is maximized when the period of the applied field is equal to the relaxation time, satisfying the resonance condition. At resonance

$$\omega\tau_m = 1$$

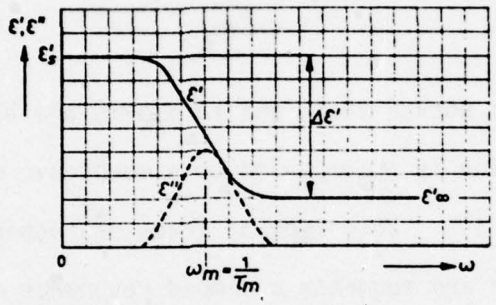


Figure 3-7: Frequency dependence of complex permittivity in the microwave region.

and

$$\varepsilon'_R = \frac{\varepsilon'_s + \varepsilon'_\infty}{2}$$

$$\varepsilon''_R = \frac{\varepsilon'_s - \varepsilon'_\infty}{2}$$

$$\tan \delta = \frac{\varepsilon'_s - \varepsilon'_\infty}{\varepsilon'_s + \varepsilon'_\infty} .$$

It is important to notice that, unlike atomic and electron polarization, dipole polarization is accompanied by a monotonic decrease in $\varepsilon'_R$, as was shown in Figure 3-5. This type of frequency dependence is known as anomalous dispersion and suggests a damped resonance due to "internal friction" effects [12]. The electrical equivalent circuit describing this type of resonance is shown in Figure 3-8. The frequency dependence of the complex permittivity in the region of dipole polarization can also

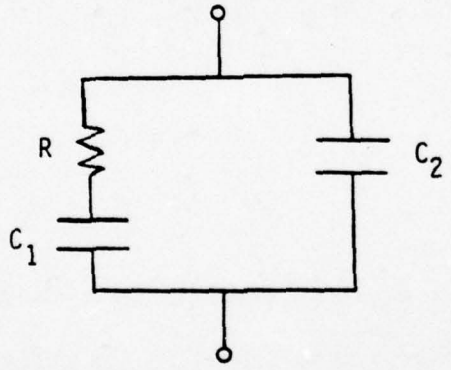


Figure 3-8: Equivalent electrical circuit describing dipole dispersion.

be viewed in the complex plane resulting in the Cole-arc diagram of Figure 3-9 [16].

Debye [15] also showed that the relaxation time is inversely related to the dielectric temperature. This temperature dependence can be

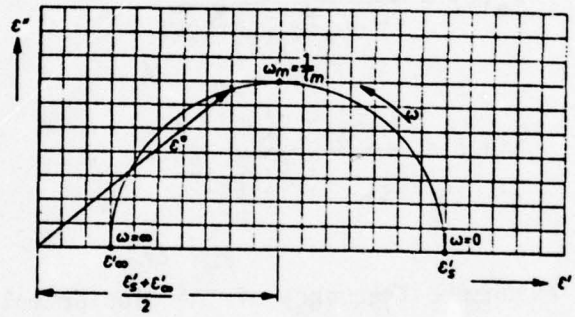


Figure 3-9: Complex permittivity diagrammed in the complex plane.

expressed as

$$\tau_m = \frac{\xi}{2kT} .$$

Equations (III-9) through (III-11) then become

$$\varepsilon'_R(\omega) = \varepsilon'_\infty + \frac{\varepsilon'_s - \varepsilon'_\infty}{1 + \omega^2(\frac{\xi}{kT})^2} \qquad \text{(III-12)}$$

$$\varepsilon''_R(\omega) = \frac{(\varepsilon'_s - \varepsilon'_\infty)\omega\xi}{(1 + \omega^2(\frac{\xi}{2kT})^2)2kT} \qquad \text{(III-13)}$$

$$\tan\delta = \frac{(\varepsilon'_s - \varepsilon'_\infty)\omega\xi}{\varepsilon'_s + \varepsilon'_\infty\omega^2(\frac{\xi}{2kT})^2} . \qquad \text{(III-14)}$$

Note that the natural resonance frequency of the dipolar molecules increases with temperature

$$\omega_m = \frac{1}{\tau_m} = \frac{2kT}{\xi} .$$

The typical behavior of $\varepsilon'_R$ and $\varepsilon''_R$ with frequency and temperature is shown in Figure 3-10. Note that at a constant frequency, $10^9$Hz for instance, the behavior may be such that the values of the parameters may even oscillate as a function of temperature.

Thus the complex permittivity and, therefore, the dielectric constant and loss tangent, are nonlinear functions of frequency and temperature. This is of extreme importance since it implies the rate of microwave heating will change with the sample temperature. This concept will be developed fully in the next section.

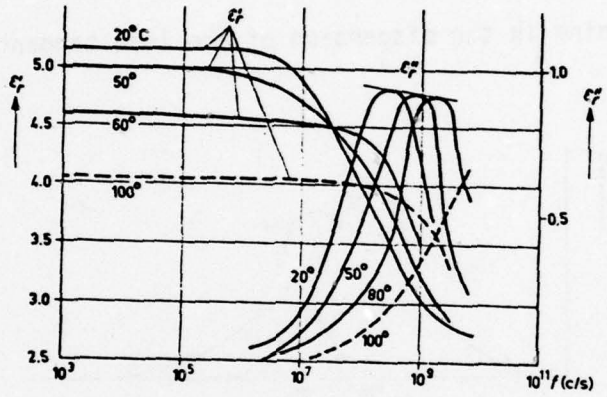


Figure 3-10: Temperature dependence of complex permittivity of a dipolar material (after Puschner [12]).

In the curing of epoxy resins by microwave heating, many different dipole species exist in the material simultaneously. It is therefore necessary to consider the effect of multiple dipolar species on the complex permittivity. Generally, the dielectric properties appear as a superposition of the behavior of each contributing type of dipole [12]. The behavior of the loss tangent of a material composed of two dipole species having different relaxation times is shown in Figure 3-11. The result is a broadening in the dispersion of the loss tangent due to the

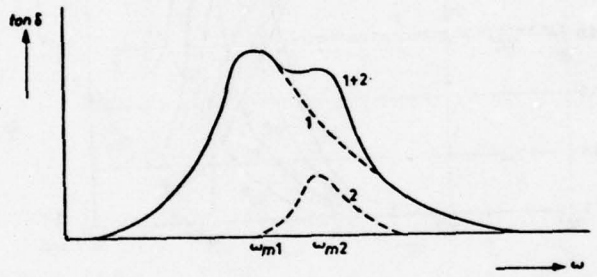


Figure 3-11: Loss tangent of a material having two dipolar species.

superposition of the losses from each species. Thus it is expected that the loss tangent of the epoxy resins, composed of multiple dipole species, will display broad dispersion.

It is important to realize that the foregoing discussion assumes no interaction of the individual dipole moments present in the dielectric. In the case of disordered solids and viscous liquids, these interactions were taken into account by Onsager [17] through his consideration of a reaction field produced by the dipole and effecting the surrounding polarized material. This appears as an additional contribution to the

previously discussed local field $\vec{E}'$. This results in a further broadening of the dispersion relations which may be considered to consist of several absorption periods $d\tau_m$ (Figure 3-12). The complex permittivity is then expressed through the relations

$$\varepsilon_R'(\omega) = \varepsilon_\infty' + \int_0^\infty \frac{f(\tau_m)d\tau_m}{1+\omega^2\tau_m^2}$$

$$\varepsilon_R''(\omega) = \int_0^\infty \frac{f(\tau_m)\omega\tau_m d\tau_m}{1+\omega^2\tau_m^2}$$

where $f(\tau_m)$ gives the distribution of the dispersion [12].

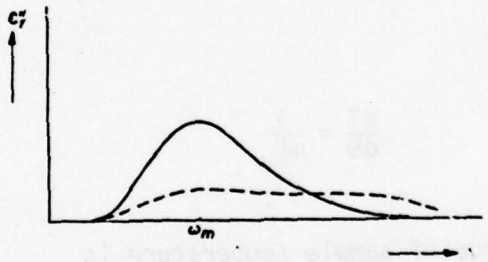


Figure 3-12: Dispersion of dielectric loss due to interactions of dipole species. Dotted line shows dispersion broadening due to Onsager field.

Thus, it is apparent that the complex permittivity, and the associated properties, are complicated, nonlinear functions of frequency and temperature. In the case of epoxy resins, this behavior is further complicated because of the number of dipolar species present in the material and because the concentration of these species change during

cure. The loss tangent of an epoxy is expected to have a broad, relatively flat dispersion and to change considerably during cure.

The Microwave Heating Equation

Now that the macroscopic parameters of interest, both material and field dependent, have been discussed, it is appropriate to describe microwave heating in terms of these variables. This will be accomplished by developing an equation relating the time rate of change in dielectric temperature to these parameters.

The specific heat at constant volume of a material is defined as

$$C_V = \frac{1}{m}\frac{dU}{dT} ,$$

where m, U, and T are the sample mass, internal energy, and temperature, respectively. Therefore,

$$\frac{dT}{dU} = \frac{1}{mC_V}$$

and the time rate of change of sample temperature is

$$\frac{dT}{dt} = \frac{dT}{dU}\frac{dU}{dt} = \frac{1}{mC_V}\frac{dU}{dt} . \qquad \text{(III-15)}$$

The quantity $\frac{dU}{dt}$ is the rate of absorption of energy by the material and is equivalent to the power dissipated in the sample. Assuming the material is ohmic, the instantaneous electric power dissipated per unit volume of material is

$$P = \vec{J}\cdot\vec{E} = \sigma\vec{E}\cdot\vec{E} = \sigma E^2 ,$$

where $\vec{J} = \sigma\vec{E}$

is the current density, E is the magnitude of the electric field, and $\sigma$ is the conductivity of the material. This conductivity term accounts for all electrical losses in the material. The instantaneous power dissipated in a sample of volume $V_S$ is then

$$\frac{dU}{dt} = V_s \sigma E^2,$$

assuming the electric field is uniform over this volume. Substituting into equation (III-15) yields

$$\frac{dT}{dt} = \frac{\sigma V_s}{mC_v} E^2.$$

The change in temperature after an irradiation time t is, therefore,

$$\Delta T = T - T_o = \int_{T_o}^{T} dT = \frac{V_s \sigma}{mC_v} \int_o^t E^2 dt.$$

Let the alternating electric field in the sample be of the form

$$E = E_o \sin \omega t.$$

Then,

$$\Delta T = \frac{V_s \sigma E_o^2}{mC_V} \int_o^t \sin^2 \omega t dt$$

$$= \frac{V_s \sigma E_o^2}{mC_V} \left(\frac{1}{2}t - \frac{1}{4\omega} \sin 2\omega t\right). \qquad \text{(III-16)}$$

However, since interest is in microwave frequencies for which $\omega$ is approximately $10^9$, the second term of equation (III-16) is on the order

of $10^{-9}$ and, therefore, for physically significant times,

$$\Delta T = \frac{V_s \sigma E_o^2}{2mC_V} t. \qquad \text{(III-17)}$$

Equation (III-17) can be written

$$T = \frac{V_s \sigma E_o^2}{2mC_V} t + T_o.$$

Differentiation yields

$$\frac{dT}{dt} = \frac{V_s \sigma E_o^2}{2mC_V} \qquad \text{(III-18)}$$

It is now necessary to express equation (III-18) in terms of the complex permittivity. This is accomplished by the relation [13]

$$\sigma = \omega \varepsilon_o \varepsilon_R''. \qquad \text{(III-19)}$$

Thus by equation (III-11),

$$\sigma = \omega \varepsilon_o \varepsilon_R' \tan \delta = \omega \varepsilon \tan \delta,$$

where

$$\varepsilon = \varepsilon_o \varepsilon_R'.$$

Therefore,

$$\frac{dT}{dt} = \frac{\omega V_s E_o^2}{2mC_V} \varepsilon(T) \tan \delta(T), \qquad \text{(III-20)}$$

where the temperature dependence of the dielectric constant and loss tangent are noted. Equation (III-20) is the heating equation expressing the rate of temperature change of a dielectric in terms of macroscopic parameters. Recall that $E_o$ is the magnitude of the field in the material

and is assumed uniform throughout the sample. These considerations will be discussed in later chapters.

Before concluding this chapter, it is necessary to consider the decrease of incident electric field energy due to losses in the material. As an electromagnetic wave passes through the dielectric of finite conductivity, the magnitude of the electric field decreases since energy is transferred from the field to the material. The "depth of penetration" is defined as the thickness of dielectric that reduces the magnitude of the field in the material by a factor of 1/e (e = 2.71828). The depth of penetration $\Delta$ is given by [13]

$$\Delta = \left(\frac{2}{\mu_o \varepsilon_o \varepsilon_R' \omega^2 \tan\delta}\right)^{\frac{1}{2}} \qquad \text{(III-21)}$$

where $\mu_o$ is the permeability of free space. It will be shown that the value of $\Delta$ for the epoxy resins is sufficiently large to be of little consequence in their microwave heating.

This chapter has developed the theory of dielectric losses in the microwave frequency region. The temperature and frequency dependence of the important dielectric parameters were then considered. Finally, a general equation describing the heating phenomenon in a dielectric irradiated by a microwave field was derived. Subsequent chapters deal with the actual measurement of complex permittivity, use of this data to quantitatively predict the heating of the epoxy resins studied, and comparison of actual heating measurements with these predictions.

# CHAPTER IV

## MEASUREMENT OF DIELECTRIC PROPERTIES

### Methodology

Analysis of the radio frequency heating behavior of the epoxy resins requires the measurement of the dielectric constant and loss tangent of the materials. Required as functions of both frequency and temperature, these measurements were made in the frequency range of 1.0 to 2.5 GHz and from 25 to 85 degrees Celsius at 1.5 GHz. A precision slotted coaxial transmission line was used to measure the null shift and voltage standing wave ratio (VSWR) associated with the standing wave pattern produced by termination of the line with the sample and a variable short. This data is used with the transmission line equations and the field equations for a lumped capacitive load to calculate sample admittance [18]. Samples of gelled, partially cured epoxy in the form of thin disk parallel plate capacitors permitted solution for the complex permittivity using the appropriate field equations.

A parallel plate capacitor sample of thickness T and surface area A is placed between the center conductor and the variable short of the sample holder shown in Figure 4-1. The sample is made very thin in order to avoid fringing effects. The electrical equivalent of this capacitive circuit is shown in Figure 4-2. The currents $I_g$ and $I_c$ are the dissipative and reactive currents, respectively. The development that follows results in a procedure for calculating complex permittivity from

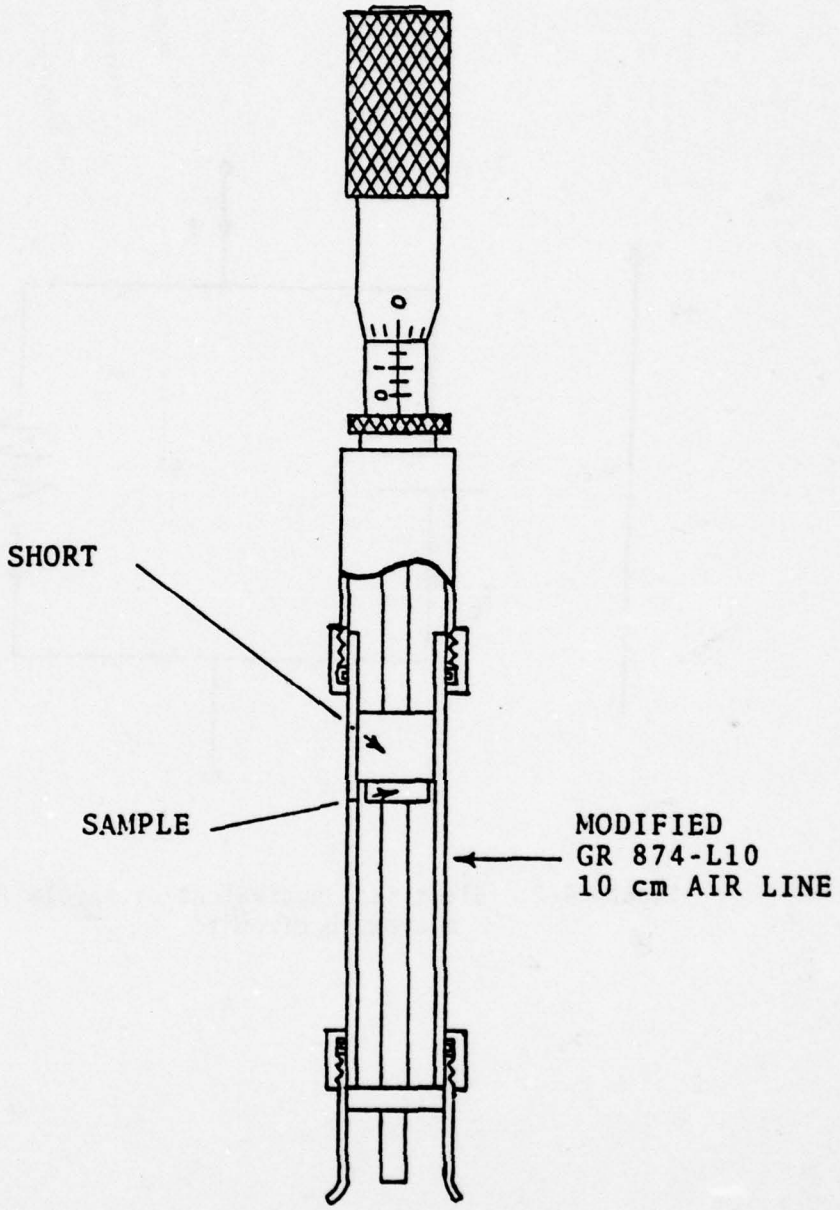


Figure 4-1: Sample holder used for complex permittivity measurements (courtesy of Mr. R. S. Rea).

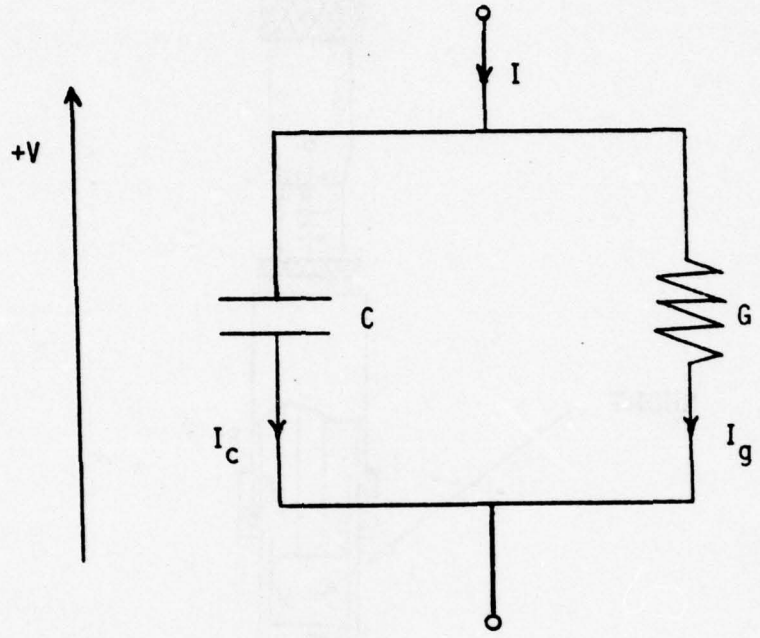


Figure 4-2: Electrical equivalent of sample in microwave circuit.

measurable parameters and is based on the treatment given by Pearson [19].

The current through a capacitor due to an applied voltage V can be expressed as

$$I = I_g + I_c = YV = (G + j\omega C)V = (G + jB)V \qquad \text{(IV-1)}$$

The corresponding electric field strength and current density are, respectively,

$$E = \frac{V}{T} \qquad \text{(IV-2)}$$

and

$$J = \frac{I}{A} . \qquad \text{(IV-3)}$$

By Maxwell's Equations, these two parameters are related through the constitutive equation

$$J = (\sigma_o + \omega\varepsilon'' + j\omega\varepsilon')E, \qquad \text{(IV-4)}$$

where $(\sigma_o + \omega\varepsilon'')E$ is the conduction current component and $j\omega\varepsilon'E$ is the displacement current component [20]. Combining equations (IV-2), (IV-3), and (IV-4), the total current is written as

$$I = (\sigma_o + \omega\varepsilon'' + j\omega\varepsilon') \frac{A}{T} V. \qquad \text{(IV-5)}$$

The admittance of the capacitive load is expressed by combining equations (IV-1) and (IV-5):

$$Y = G + jB = G + j\omega C = (\sigma_o + \omega\varepsilon'' + j\omega\varepsilon') \frac{A}{T}. \qquad \text{(IV-6)}$$

Equating real and imaginary terms of equation (IV-6) results in, respectively, the conductance

$$G = (\sigma_o + \omega\varepsilon'') \frac{A}{T} \qquad \text{(IV-7)}$$

and the susceptance

$$B = \omega\varepsilon' \frac{A}{T} . \qquad \text{(IV-8)}$$

For the materials under consideration the first term of equation (IV-7) is negligible, the total conductivity being given by equation (III-19). Thus, the dielectric forming the capacitor has as the components of its complex permittivity

$$\varepsilon_R' = \frac{BT}{\varepsilon_o \omega A} \qquad \text{(IV-9)}$$

and

$$\varepsilon_R'' = \frac{GT}{\varepsilon_o \omega A}. \qquad \text{(IV-10)}$$

By definition, the loss tangent is

$$\tan\delta = \frac{\varepsilon''}{\varepsilon'} = \frac{G}{B}. \qquad \text{(IV-11)}$$

The dielectric parameters of interest have been related to the conductance and susceptance of an electric circuit in which the material is a capacitive load. Now it is necessary to measure these electrical parameters, indirectly, and compute the dielectric parameters. This is accomplished by measuring the voltage along a slotted coaxial transmission line terminated by the load.

Consider a transmission line as shown in Figure 4-3, with input admittance $Y_{IN}$ and terminated by a load $Y_L$. The incident and reflected voltages $V^+$ and $V^-$, respectively, result in a sinusoidal standing wave pattern along the line. The voltage along the line a distance $\ell$ from the load is given as

$$V = V^+ e^{j\beta\ell} + V^- e^{-j\beta\ell},$$

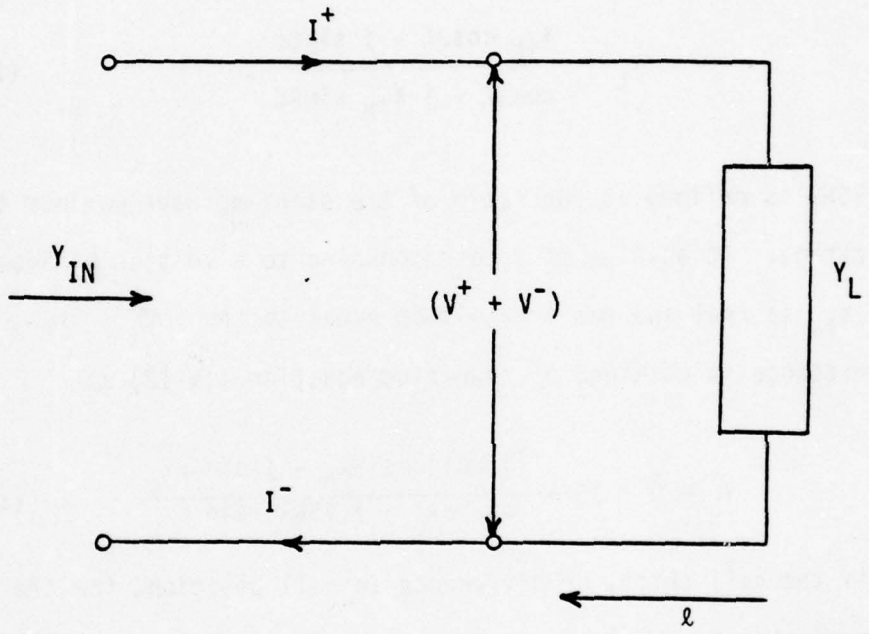


Figure 4-3: Transmission line terminated in load $Y_L$.

where $$\beta = \frac{2\pi}{\lambda}$$

is the propagation constant. Similarly, the current along the line is

$$I = I^{+}e^{j\beta\ell} - I^{-}e^{-j\beta\ell}.$$

It is shown by Pearson [19] that the admittance of the load is given by

$$Y_L = \frac{Y_{IN}\cos\beta\ell - j\sin\beta\ell}{\cos\beta\ell - j\,Y_{IN}\sin\beta\ell}. \qquad \text{(IV-12)}$$

The VSWR is defined as the ratio of the standing wave maximum to minimum voltage. At a value of $\ell$ corresponding to a voltage minimum the value $Y_{IN}$ is real and has a magnitude equal to the VSWR. Thus, the sample admittance is obtained by rewriting equation (IV-12) as

$$Y_L = G + jB = \frac{(\text{VSWR})\cos\beta x_o - j\sin\beta x_o}{\cos\beta x_o - j(\text{VSWR})\sin\beta x_o}, \qquad \text{(IV-13)}$$

where $x_o$ is the null shift, or difference in null position, for the circuit terminated by the load and by a short [21]. This null shift, due to the effective electrical length of the sample, is a result of the radiation having a different wavelength in the sample than in air.

The process of computing the components of the complex permittivity involves measuring the wavelength in air, VSWR, and null shift. The admittance and susceptance are then found as the real and imaginary parts of equation (IV-13), respectively. The relative dielectric constant and loss tangent are then computed using the capacitor equations (IV-9) and (IV-11), respectively. These computations are performed with the aid of the computer program SLOT2, given in Appendix I. This lumped

capacitance technique is considered valid up to approximately 3 GHz and has been used successfully to 2.5 GHz [22,23].

Experimental Procedure

Gelled epoxy resins supplied by AMMRC were cut, using a diamond core borer, and polished to form thin, disk-shaped samples. The disks made by this method had flat, parallel faces and were approximately 6 mm in diameter and 0.5 mm thick. Following measurement of their dimensions, the disk faces were coated with silver conducting paint, forming a parallel plate capacitor. This sample could then be placed between the center conductor of a coaxial air line and a short circuit termination. This circuit configuration satisfies the conditions for analysis by the techniques described in the preceeding section.

The apparatus for measuring the dielectric properties is diagrammed in Figure 4-4. The output of a microwave signal generator was sine wave

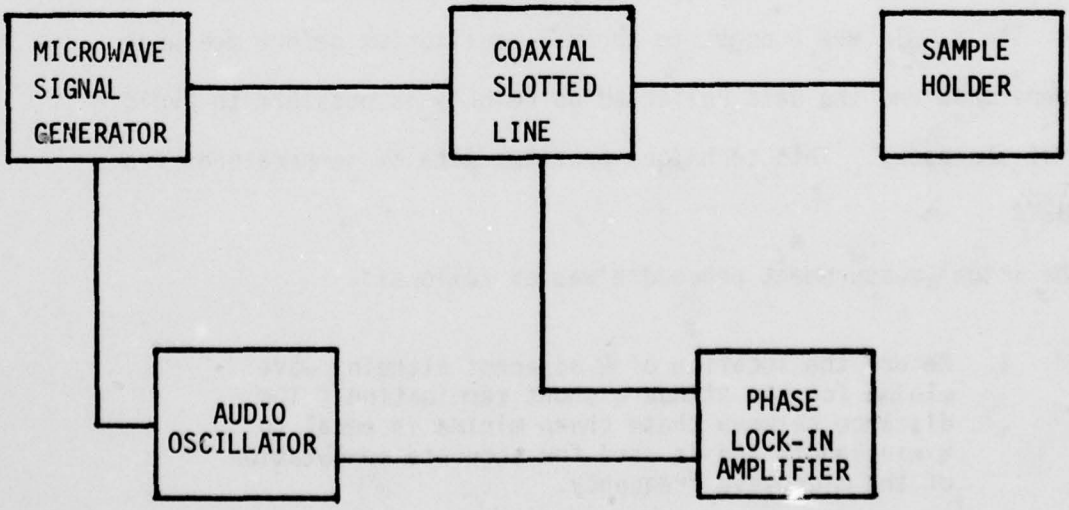


Figure 4-4: Block diagram of complex permittivity measurement apparatus.

modulated at 1 KHz by an audio oscillator and input to a precision coaxial slotted line. The voltage out of the detector diode was input to a phase-locked-loop amplifier referenced to the 1 KHz modulation signal. The sample holder, shown in Figure 4-1, was equipped with an electric heater coil and thermocouple fastened to the outer conductor.

The lock-in amplifier was used as a voltmeter in order to measure the VSWR. The loss tangent of the epoxies is such that the VSWR of the capacitor samples is too high to measure with a conventional standing wave meter. Using the lock-in amplifier, the voltage at the standing wave maxima and minima is measured directly. The VSWR is calculated as their ratio. This instrument permitted voltage measurements on the order of a nanovolt.

Thermal dependence of the complex permittivity was measured by connecting a d.c. power supply to the heater coil and adjusting the voltage until thermal stability was achieved. Sample temperature was measured with a copper/constantan thermocouple attached to the sample holder. The sample was brought to thermal equilibrium before measurements were made and the data collected as quickly as possible to avoid curing of the epoxy. This technique provided data at temperatures from 25 to 85$^{o}$C.

The actual measurement procedure was as follows:

1. Record the location of 2 adjacent standing wave minima for the standard short termination. The distance between these sharp minima is equal to ½ wavelength and is used for accurate computation of the microwave frequency.

2. Replace the standard short with the loaded sample holder and record the new position of one of the

minima from step 1. This distance between minima is the null shift.

3. Record the voltage at the node located in step 2.

4. Record the voltage at the maxima adjacent to this node and compute their average.

5. Compute the VSWR as the quotient of this average voltage and the voltage measured in step 3.

The position measurements along the slotted line were made to 0.1 mm accuracy. The two node locations from step 1, the node location from step 2, and the VSWR from step 5 are required input data for the computer program SLOT2. From this data, and the sample disk diameter and thickness, the relative dielectric constant and loss tangent are computed.

Results

Complex permittivity measurements were made on two of the four types of epoxy resins supplied by AMMRC. These were the gelled 828-T403 and 828-Z resin/curing agent systems. The other gelled resins supplied were found to be brittle and unsuitable for sample fabrication. The relative dielectric constant and loss tangent were computed by the procedure described in the previous section.

The relative dielectric constant and loss tangent of the gelled 828-T403 resin is given in Figures 4-5 and 4-6, respectively. Similar data for gelled 828-Z resin is shown in Figures 4-7 and 4-8. These figures present data taken at 23, 60, and 70 degrees Celsius over the frequency range 1.0 to 2.5 GHz. The straight lines through the $\varepsilon_R'$ curves give the average value of the measurements and, essentially, are a least squares fit to a constant value. The constant value of $\varepsilon_R'$ is expected,

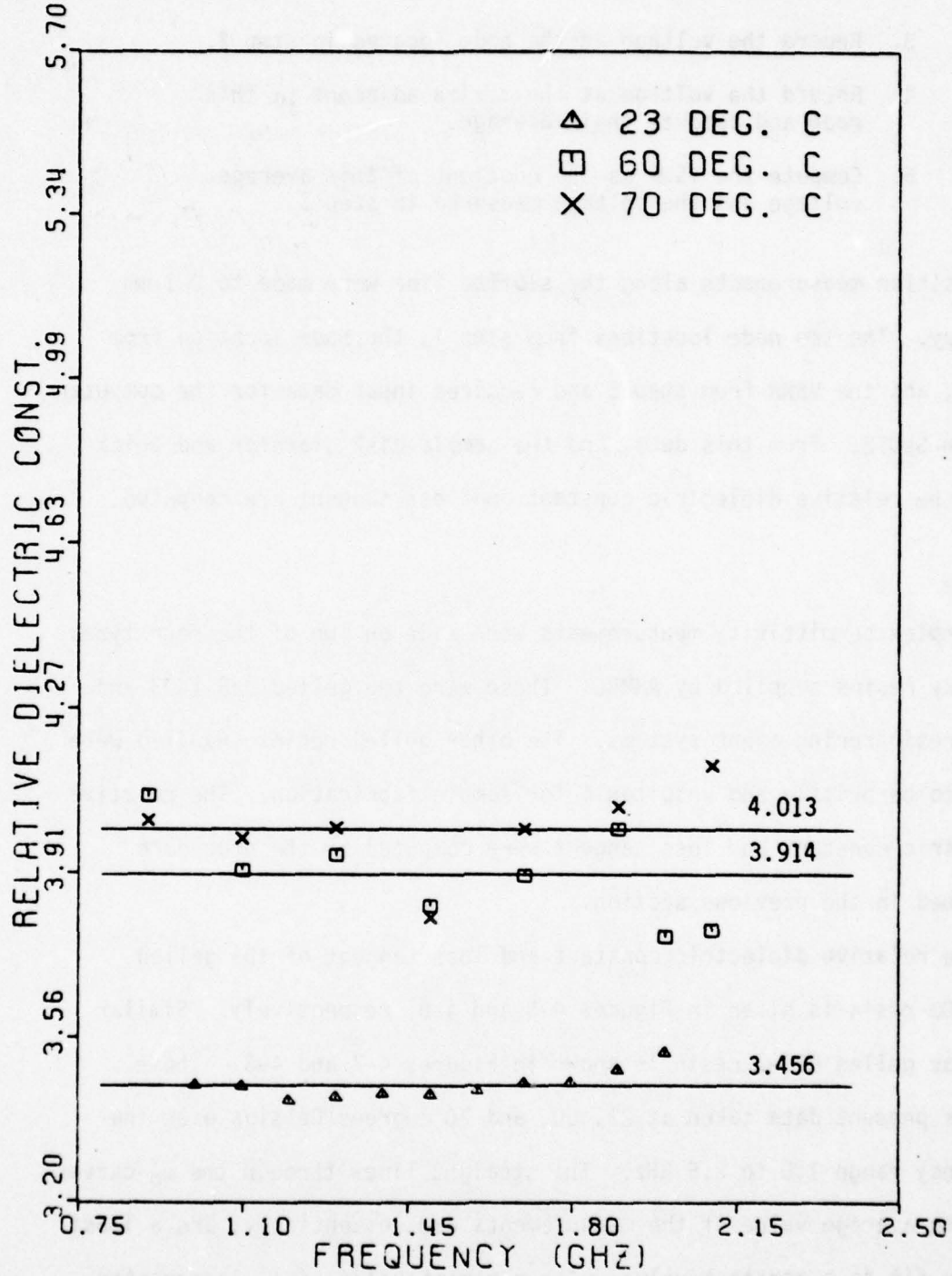


Figure 4-5: Relative dielectric constant of gelled 828-T403 epoxy. Solid lines and numbers indicate average values.

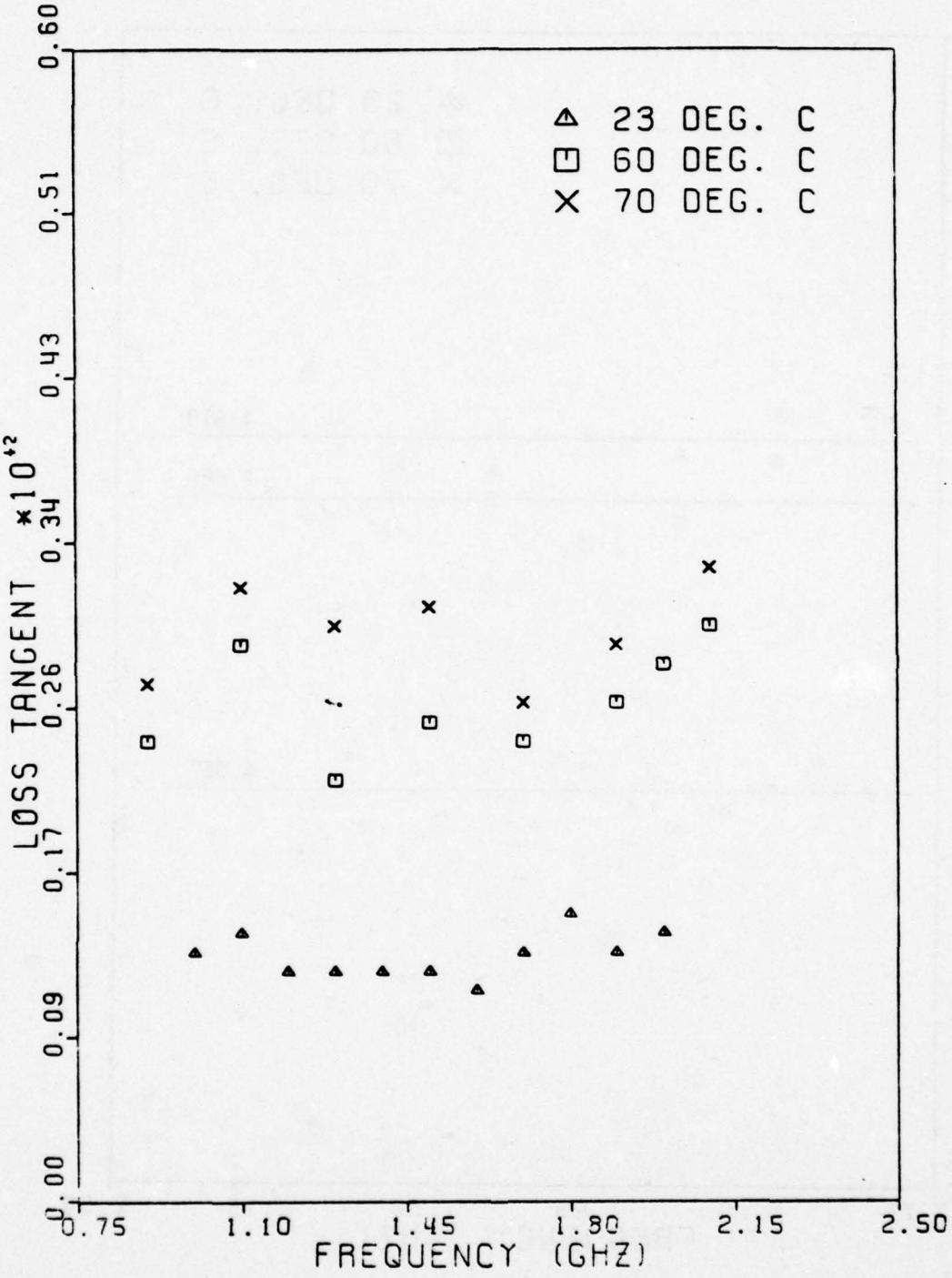


Figure 4-6: Loss tangent of gelled 828-T403 epoxy.

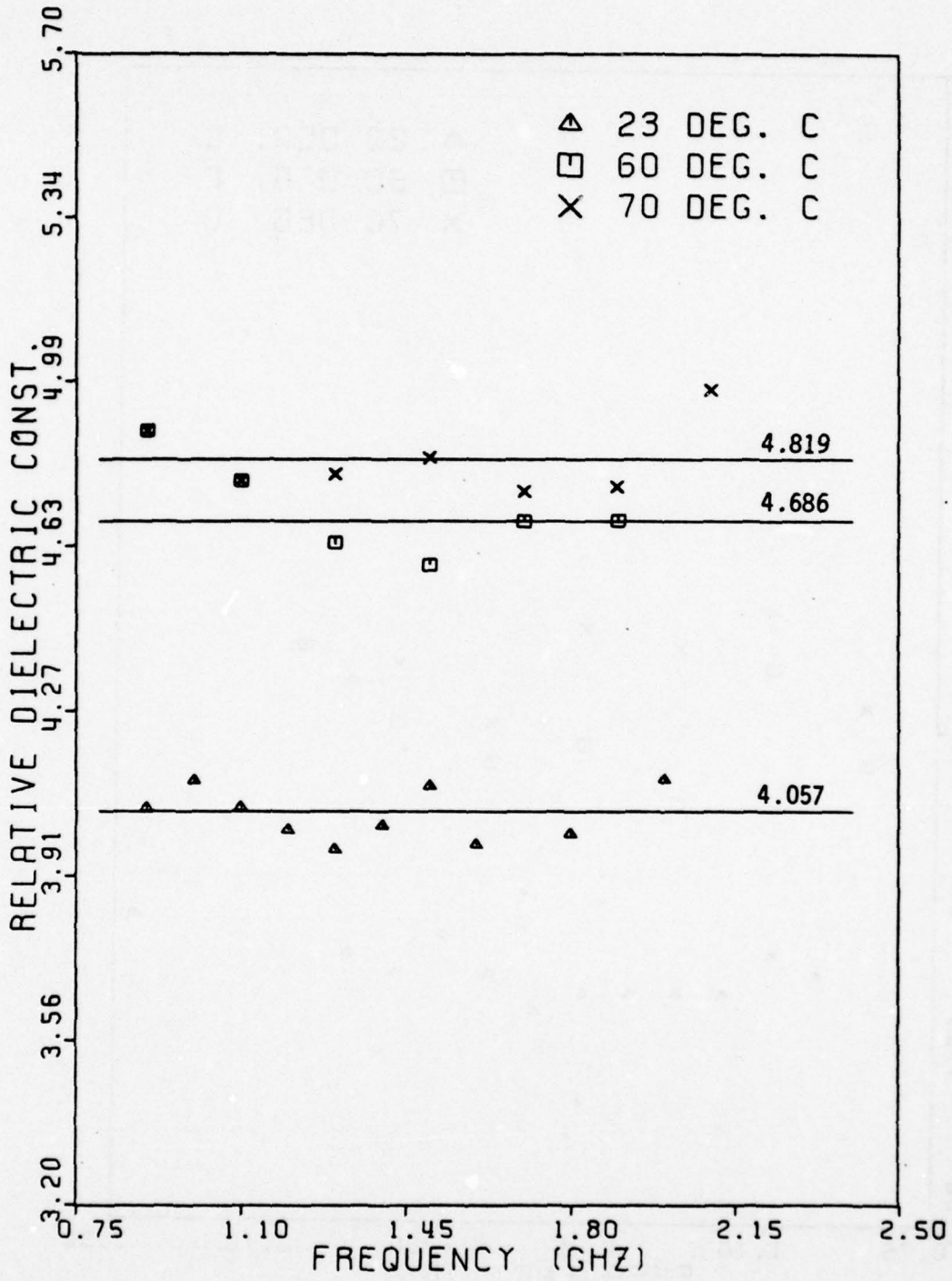


Figure 4-7: Relative dielectric constant of gelled 828-Z epoxy. Solid lines and numbers indicate average values.

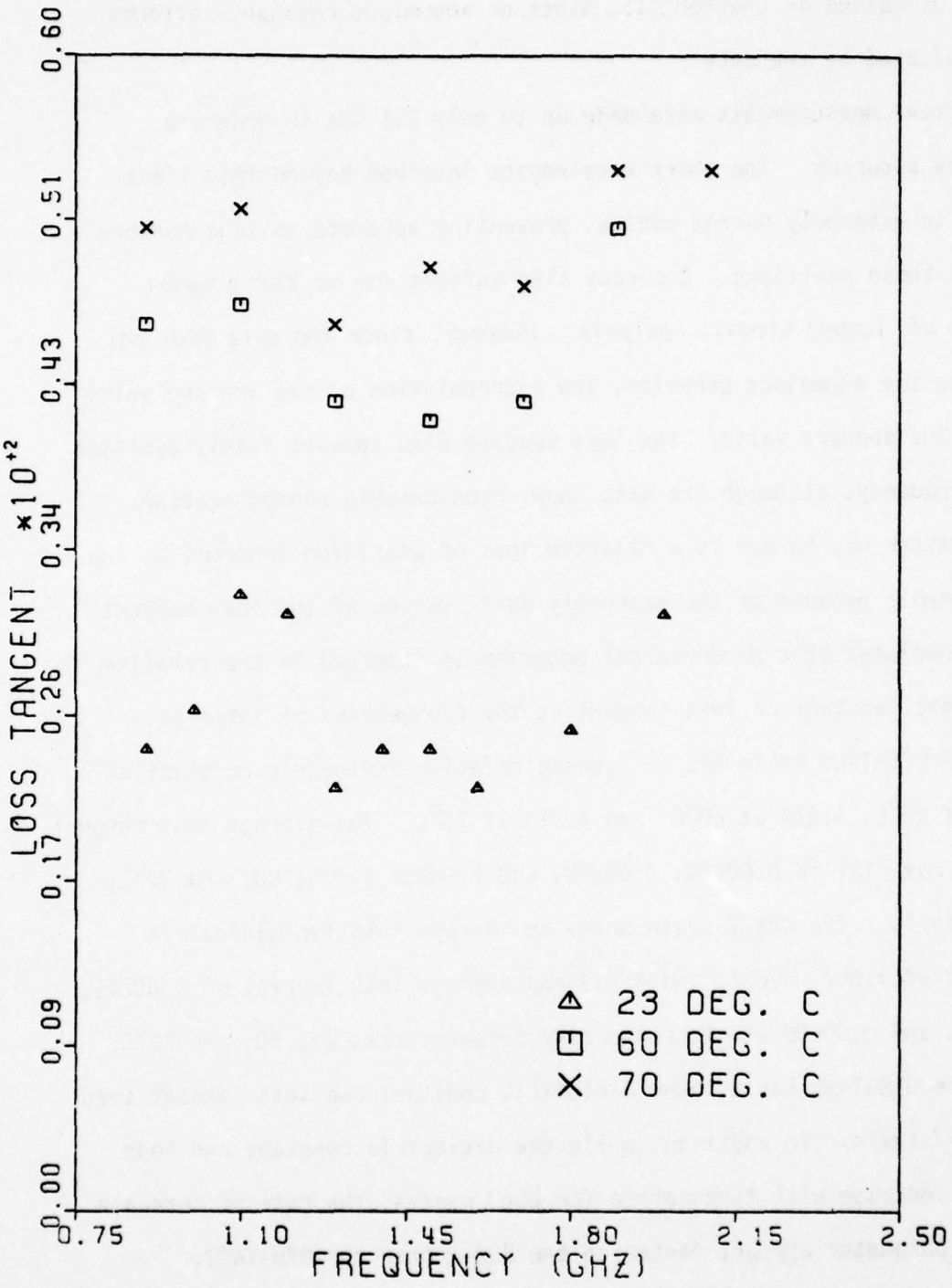


Figure 4-8: Loss tangent of gelled 828-Z epoxy.

as was discussed in Chapter III, since no anomalous resonance effects are indicated by the data.

Actual measurements were made up to only 2.1 GHz in order to preserve accuracy. The short wavelengths involved beyond this limit result in extremely narrow minima, preventing accurate voltage measurement at these positions. Accuracy also suffers due to the gradual failure of lumped circuit analysis. However, since the data does not indicate any anomalous behavior, the extrapolation of the average value to 2.5 GHz appears valid. The loss tangent also appears fairly constant with frequency, although the data shows considerable random scatter. This scatter may be due to a relative loss of precision inherent in the measurements because of the extremely small values of the loss tangent. It is concluded that no anomalous behavior is observed in the relative dielectric constant or loss tangent at the frequencies of interest.

The 828-T403 resin has an average relative dielectric constant of 3.456 at 23$^{o}$C, 3.914 at 60$^{o}$C, and 4.013 at 70$^{o}$C. The average loss tangent of this material is 0.00128, 0.00260, and 0.00267 at 23, 60, and 70$^{o}$C, respectively. The 828-Z resin shows an average relative dielectric constant of 4.057, 4.686, and 4.819 and average loss tangent of 0.00261, 0.00448, and 0.00506 at the respective temperatures, 23, 60, and 70$^{o}$C. Thus, the 828-T403 has a lower dielectric constant and loss tangent than the 828-Z resin. In addition, while the dielectric constant and loss tangent increase with temperature for both resins, the rate of increase of each parameter appears faster in the 828-Z than the 828-T403.

The data taken at 23$^{o}$C on the 828-T403 resin appear to be the smoothest. This is because the results are an average of four trials with

average standard deviations of 0.031 for the dielectric constant measurements and 0.0001 for the loss tangent. This averaging, although not done for all the measurements, shows that there is good repeatability in the experimental results. The smoothness of these curves is evidence that there is no anomalous behavior in the complex permittivity of the materials studied at the frequencies of interest.

Due mainly to the amount of material available for sample fabrication, most measurements were made on the 828-T403 resin. Figures 4-9 and 4-10, respectively, give the relative dielectric constant and loss tangent of cured 828-T403 in comparison with the uncured, gelled material at $23^{o}C$. Curing results in a decrease in electrical loss and an increase in dielectric constant, the average value of $\varepsilon_R'$ and $\tan\delta$ being 3.548 and 0.00103, respectively, in the cured material. This phenomena may possibly be attributed to formation of hydroxyl groups, as will be discussed later.

Chapter III demonstrated the need for measurement of complex permittivity as a function of temperature. Such a measurement was done on the 828-T403 resin, over the temperature range of 25 to $85^{o}C$, at 1.5 GHz. The choice of frequency was somewhat arbitrary, as demonstrated by the independence of dielectric constant and loss tangent with frequency, but 1.5 GHz was chosen because of ease and precision of the measurements. The experimental results are shown in Figures 4-11 and 4-12, the data normalized to the $25^{o}C$ values. Although both $\varepsilon_R'$ and $\tan\delta$ increase with sample temperature, the important feature of this behavior is the relatively large and monotonic increase in loss tangent. This means that the rate of microwave heating will increase with temperature since the loss tangent increases faster than the dielectric constant.

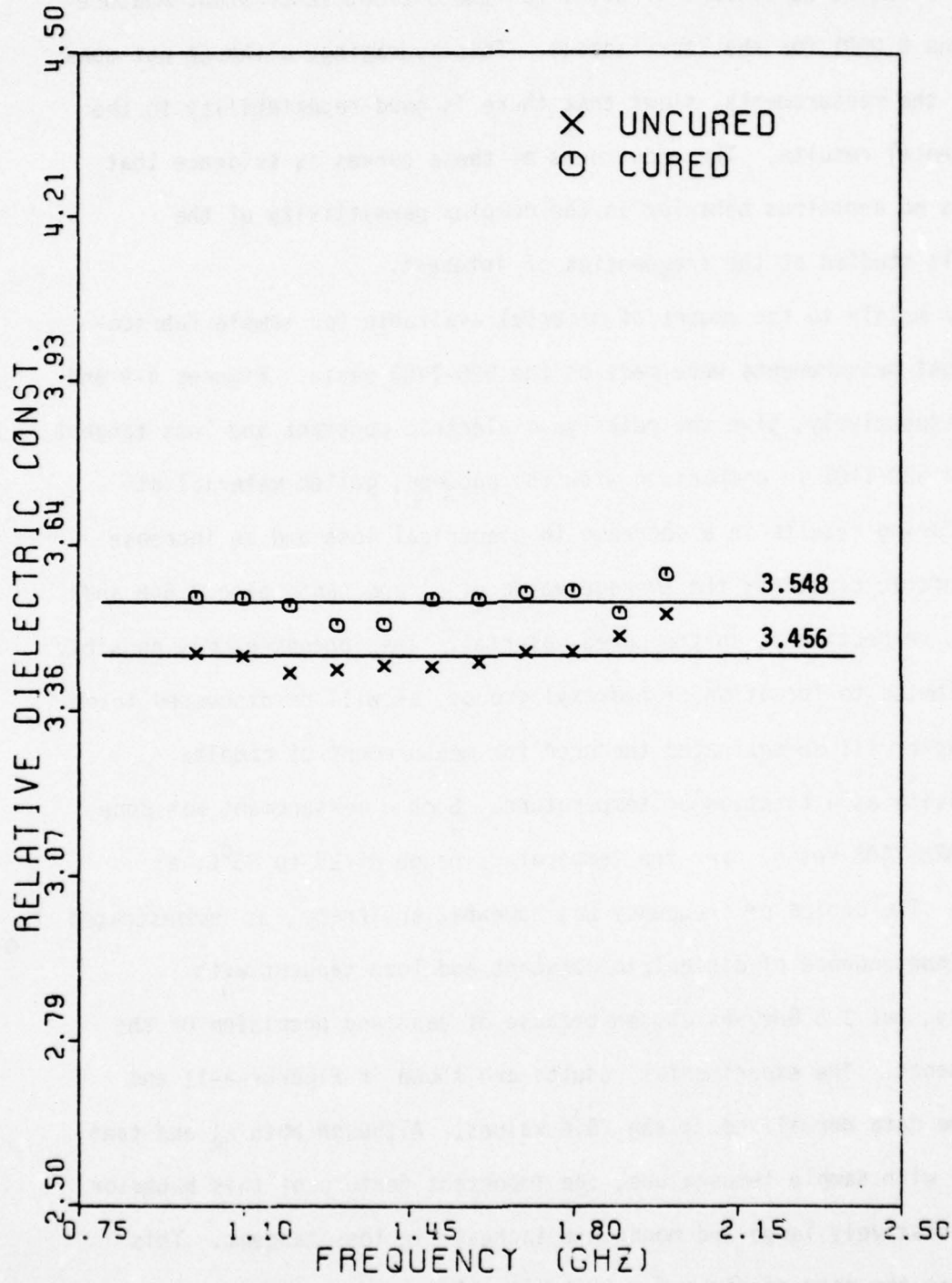


**Figure 4-9: Relative dielectric constant of cured and gelled 828-T403 epoxy. Solid lines and numbers indicate average values.**

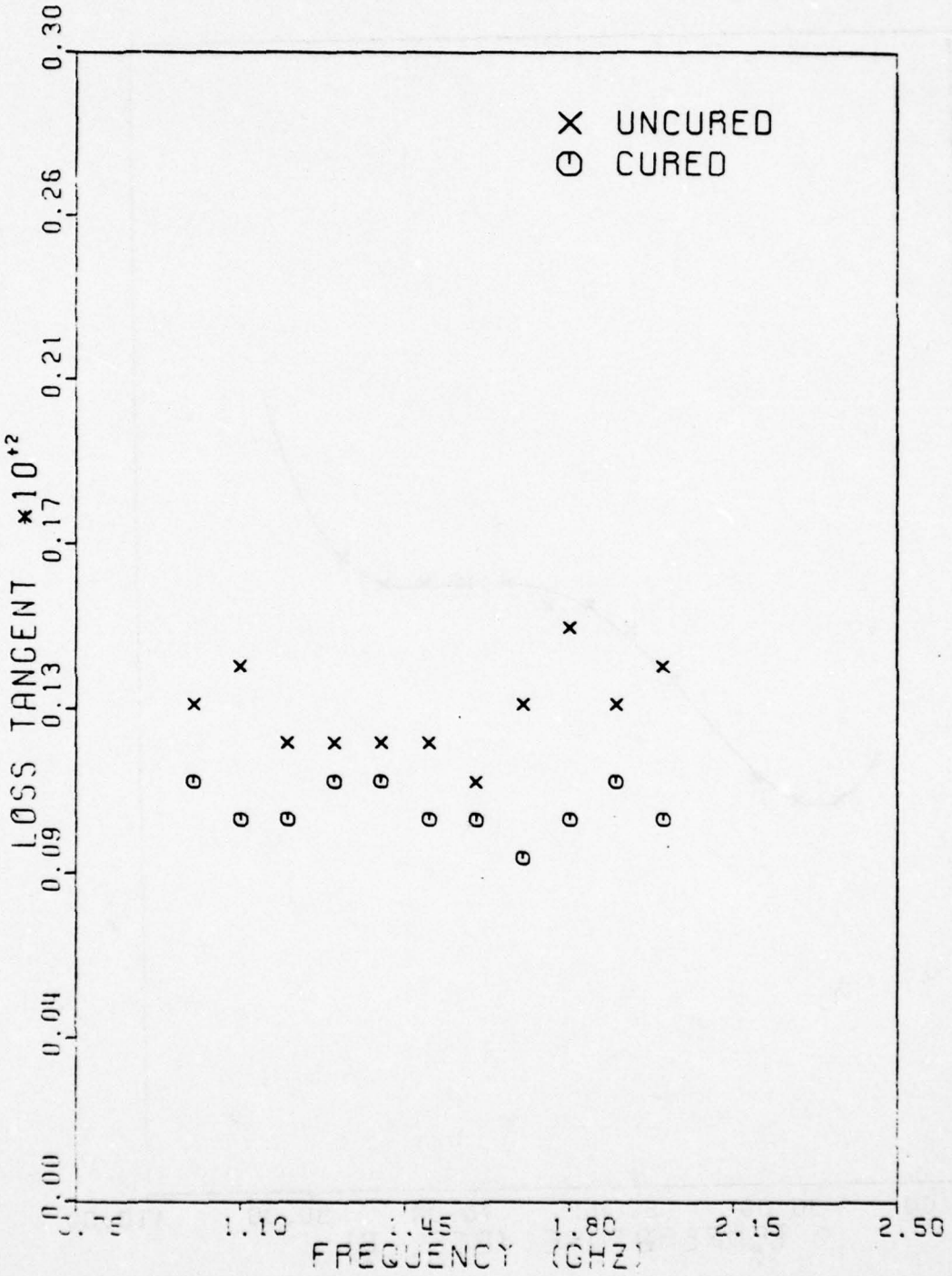


Figure 4-10: Loss tangent of cured and gelled 828-T403 epoxy.

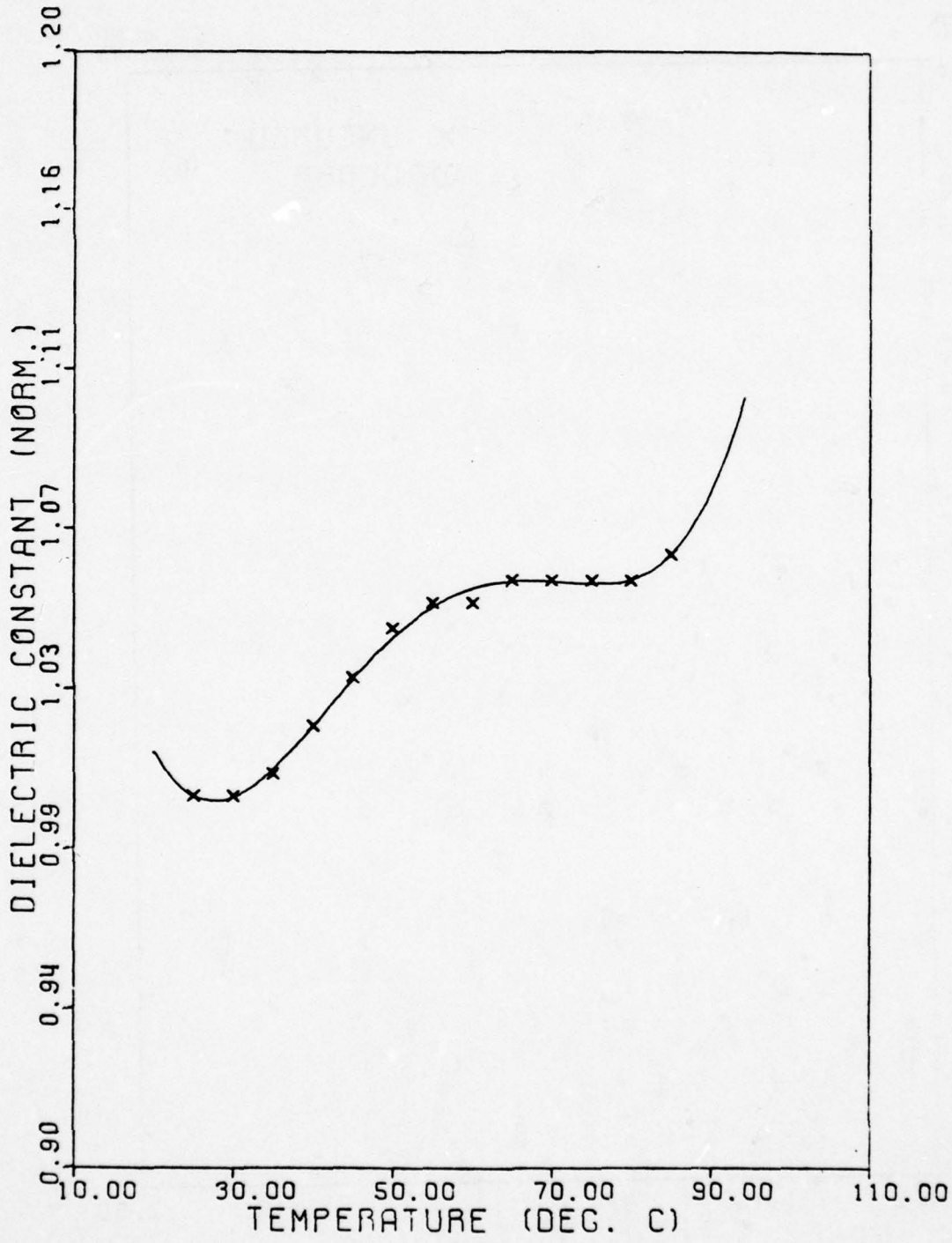


Figure 4-11: Dielectric constant of gelled 828-T403 epoxy versus temperature at 1.5 GHz. Data is normalized to the 25°C value. Solid line is a polynomial fit to the data.

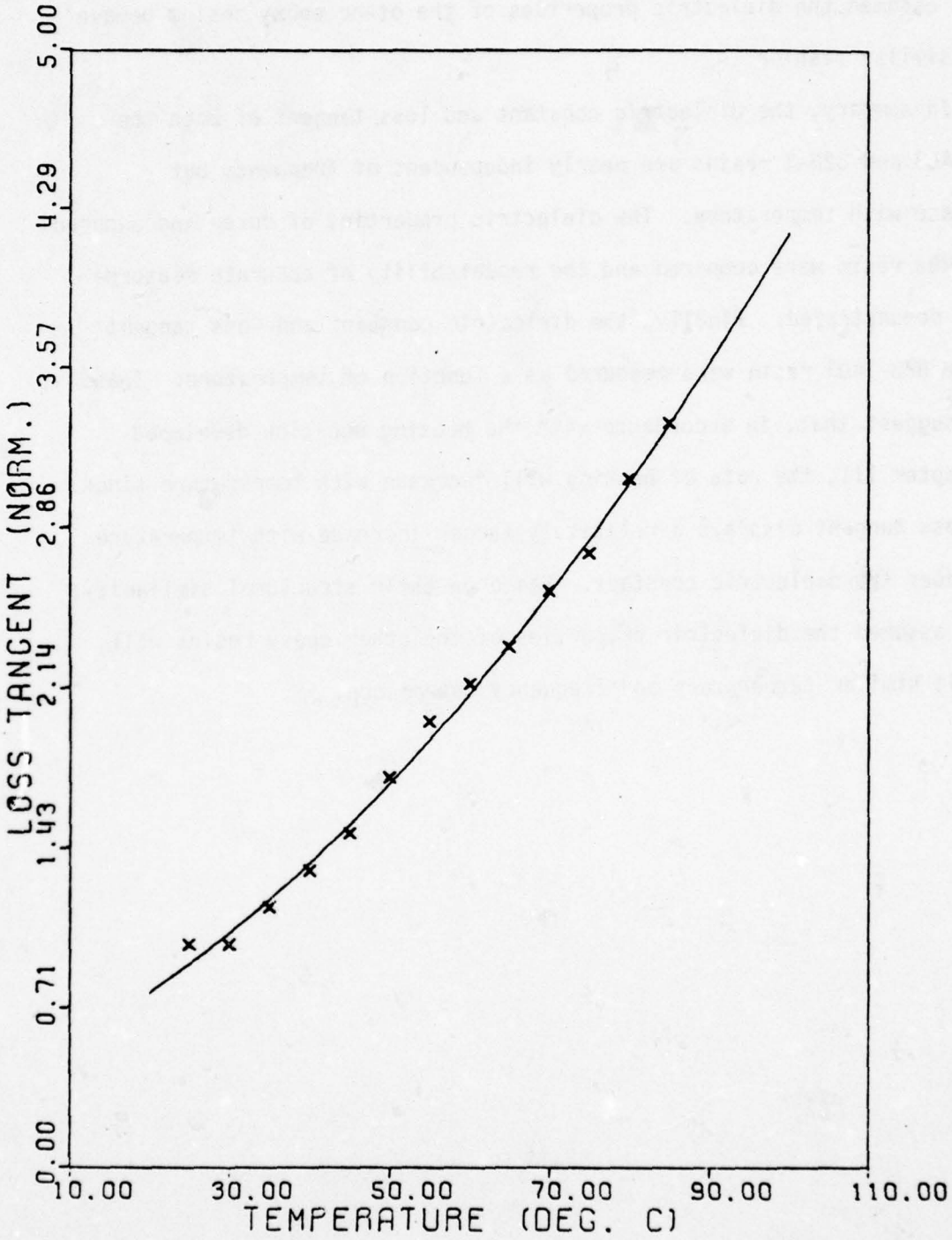


Figure 4-12: Loss tangent of gelled 828-T403 epoxy versus temperature at 1.5 GHz. Data is normalized to the 25°C value. Solid line is a polynomial fit to the data.

It is assumed the dielectric properties of the other epoxy resins behave in a similar fashion.

In summary, the dielectric constant and loss tangent of both the 828-T403 and 828-Z resins are nearly independent of frequency but increase with temperature. The dielectric properties of cured and uncured 828-T403 resin were compared and the repeatability of accurate measurements demonstrated. Finally, the dielectric constant and loss tangent of the 828-T403 resin were measured as a function of temperature. These data suggest that, in accordance with the heating equation developed in Chapter III, the rate of heating will increase with temperature since the loss tangent displays a relatively larger increase with temperature than does the dielectric constant. Based on their structural similarity, it is assumed the dielectric properties of the other epoxy resins will exhibit similar temperature and frequency dependence.

# CHAPTER V

## MICROWAVE HEATING OF EPOXY

The goal of this project is to explain the mechanisms involved in the microwave heating of liquid epoxy resins to promote a curing reaction. In order to supply the necessary background information for this explanation, previous chapters have discussed the basic chemistry of epoxies, developed an equation for the rate of microwave heating in a dielectric, and presented the dielectric properties of the epoxies pertinent to the discussion of their microwave heating. This chapter presents a theoretical model of microwave heating in the epoxies and compares these results with actual heating experiments. Explanation of the results will be based on discussions in the previous chapters.

### Microwave Heating in a Multimode Cavity

A multimode resonant cavity, such as a microwave oven, is one in which many modes of oscillation are present simultaneously. These modes superimpose to produce a standing wave pattern in the cavity. Associated with this microwave heating device are the advantages of having a uniform electric field over a large volume and high conversion efficiency of microwave power into heat [24]. The theory of mode generation in a multimode cavity is analogous to the acoustic theory presented by Bolt [25] and Maa [26]. Multimode cavity design considerations are given by Morin [27], James et al. [24], and Puschner [12]. The theory of microwave heating in this type of resonant cavity will now be

presented.

Consider an air filled resonant multimode cavity that, by design, has a uniform electric field over the central volume. If there is no dielectric load in the cavity, all power is reflected back to the source due to the total impedance mismatch. However, if the cavity contains a dielectric load, some of the power will be absorbed and converted into heat in the material. Not all the power will be absorbed since, in general, there is still an impedance mismatch. The amount of power absorbed by a dielectric of volume $V_S$ is

$$P_{LOSS} = \omega\varepsilon_0\varepsilon_R' \tan\delta E_0^2 V_S, \qquad (V\text{-}1)$$

where $E_0$ is the field amplitude in the sample and $\varepsilon_R'$ and $\tan\delta$ are the material properties [12]. The rate of heating associated with this power absorption, as derived in Chapter III, is

$$\frac{dT}{dt} = \frac{\omega V_S E_0^2}{2mC_V} \varepsilon(T) \tan\delta(T). \qquad (III\text{-}20)$$

Although the dielectric constant and loss tangent of the epoxies are known as functions of frequency and temperature, the electric field amplitude in the dielectric must also be known for equation (III-20) to be useful. Alternatively, the relation can be expressed in terms of the free space electric field. For heating in a resonant multimode cavity, it will be assumed that the electromagnetic field is, in effect, normally incident on a dielectric sample. For this condition, the electric field amplitude in the material is related to the free space amplitude $E_{0_{FS}}$ by

$$E_0 = \frac{E_{0_{FS}}}{\varepsilon_R'} . \qquad (V\text{-}2)$$

Substituting equation (V-2) into equation (III-20) gives

$$\frac{dT}{dt} = \frac{\omega V_S \varepsilon_0 E_{0_{FS}}^2}{2mC_V} \frac{\tan \delta(T)}{\varepsilon_R'(T)} . \qquad (V\text{-}3)$$

The free space amplitude $E_{0_{FS}}$ can be found by experiment, as will be discussed later.

Solution of equation (V-3) gives the rate of microwave heating in a dielectric. For the case of the epoxies, analytical expressions for $\tan \delta(T)$ and $\varepsilon_R'(T)$ have been obtained by curve fitting the experimental data. Measurement of the value of the free space electric field amplitude will be explained shortly. It is therefore possible to obtain a theoretical model of sample temperature as a function of irradiation time.

A numerical approximation for the solution of internal sample temperature as a function of irradiation time can be made using equation (V-3). Assume a sample has an initial temperature $T_0$ at time $t_0$ and let successive times $t_1$, $t_2$, $t_3$, ... have corresponding temperatures $T_1$, $T_2$, $T_3$, .... For a sufficiently small difference between successive times, $\Delta t$, the temperature at time $t_n$ is

$$T_n = (\Delta t)\frac{dT}{dt} + T_{n-1}$$

or

$$T_n = (\Delta t)\frac{\omega V_S \varepsilon_0 E_{0_{FS}}^2}{2mC_V} \frac{\tan \delta(T_{n-1})}{\varepsilon_R'(T_{n-1})} + T_{n-1}. \qquad (V\text{-}4)$$

Equation (V-4) is used in the computer program TEMPTHEORY, given in Appendix I, to provide a theoretical model of microwave heating of the epoxies with which experimental results are compared. The program uses equation (V-1) to limit the maximum power absorbed by the theoretical sample. Use of the functions describing temperature dependence of the complex permittivity was confined to valid limits.

## Experimental Microwave Heating Measurements

The microwave heating phenomena in the uncured epoxies proved quite complex. In order to explain this behavior, it was necessary to generate experimental heating curves by measuring the temperature of a sample undergoing cure by microwave heating. The high power microwave source used for these experiments was a conventional microwave oven, operated at 2.45 GHz, with two available power settings of 245 and 700 watts. The oven was modified by the introduction of a shielded thermocouple into the cavity. The thermocouple entered the cavity via a waveguide, attached to the exterior of the cavity wall, whose length and cut off frequency were sufficiently large to prevent radiation leakage at the operating frequency. The thermocouple was placed in a glass tube and inserted into the sample. Thermocouple voltage was monitored with a chart recorder during heating. This technique was used to produce the heating curves that follow.

The modeling technique discussed in the previous section was used to compare the experimental heating curves with those anticipated based on the dielectric measurements of Chapter IV. In order to accomplish this, it is necessary to measure the free space amplitude of the electric field in the oven. This was accomplished by measuring the heating curve for a

30 ml sample of distilled water. By measuring the slope of the initial, low temperature portion of this heating curve, and using the known loss tangent and dielectric constant of pure water, equation (V-3) can be solved for the free space electric field amplitude. The results of these measurements were

$$E_{0_{FS}} = 1.62 \times 10^5 \text{ V/m at } 245 \text{ W}$$

and

$$E_{0_{FS}} = 2.69 \times 10^5 \text{ V/m at } 700 \text{ W}$$

These values were used in the program TEMPTHEORY to predict the heating behavior of the epoxies.

Microwave heating in the 828-T403 and 828-Z epoxy systems was studied by this technique and the experimental results are presented in the next section. Direct microwave heating experiments were not performed on the other epoxy systems of interest. The reason for this was that no complex permittivity data was available, either from the literature or by experiment, for use in modeling the heating behavior. Since the modeling is necessary for interpretation of the experimental results, any conclusions based on these experiments would be invalid. However, based on the similarities in the general nature of epoxies, and the experimental results that are presented, it is conjectured that the conclusions drawn from these experiments apply to all four epoxy systems under consideration by AMMRC.

## Results

The experimentally determined data on microwave heating in the uncured

epoxies at 245 W, and the theoretical modeling results, are presented in Figures 5-1 through 5-3. Figures 5-1 and 5-2 show the heating of two 30 ml samples of 828-T403 epoxy while Figure 5-3 shows the heating in 30 ml of 828-Z. It is seen from these curves that the curing reaction is exothermic since the sample temperature continues to increase after the microwave source is turned off. In the case of the 828-Z epoxy (Figure 5-3), this temperature increase is dramatic. In each of these experiments, visual observation showed that the epoxy samples did not solidify until after the oven was turned off and the reaction was proceeding exothermically. In each sample, the heating was of such intensity that the samples boiled before hardening, the vapor bubbles being trapped in the solidified epoxy.

In order to illustrate the rate of change in sample temperature during the heating and curing process, Figures 5-4 through 5-6 show the slope of the heating curves given in Figures 5-1 through 5-3, respectively. Notice the rapid increase in slope at the lower temperatures, corresponding to the concave upward initial portion of the heating curve. Also note the increase in slope, due to heat produced by exothermic reaction, after the microwave source is turned off. The central portions of the heating curves appear to be of approximately constant slope or slightly concave downward.

Two model curves, designated by solid lines, are shown with the experimental curve in Figures 5-1 through 5-3. Both of these models were generated using the experimentally determined values of $\varepsilon_R'$. However, the lower, concave upward curve in each figure was obtained using the experimental values for $\tan\delta$ while the upper curve was obtained assuming

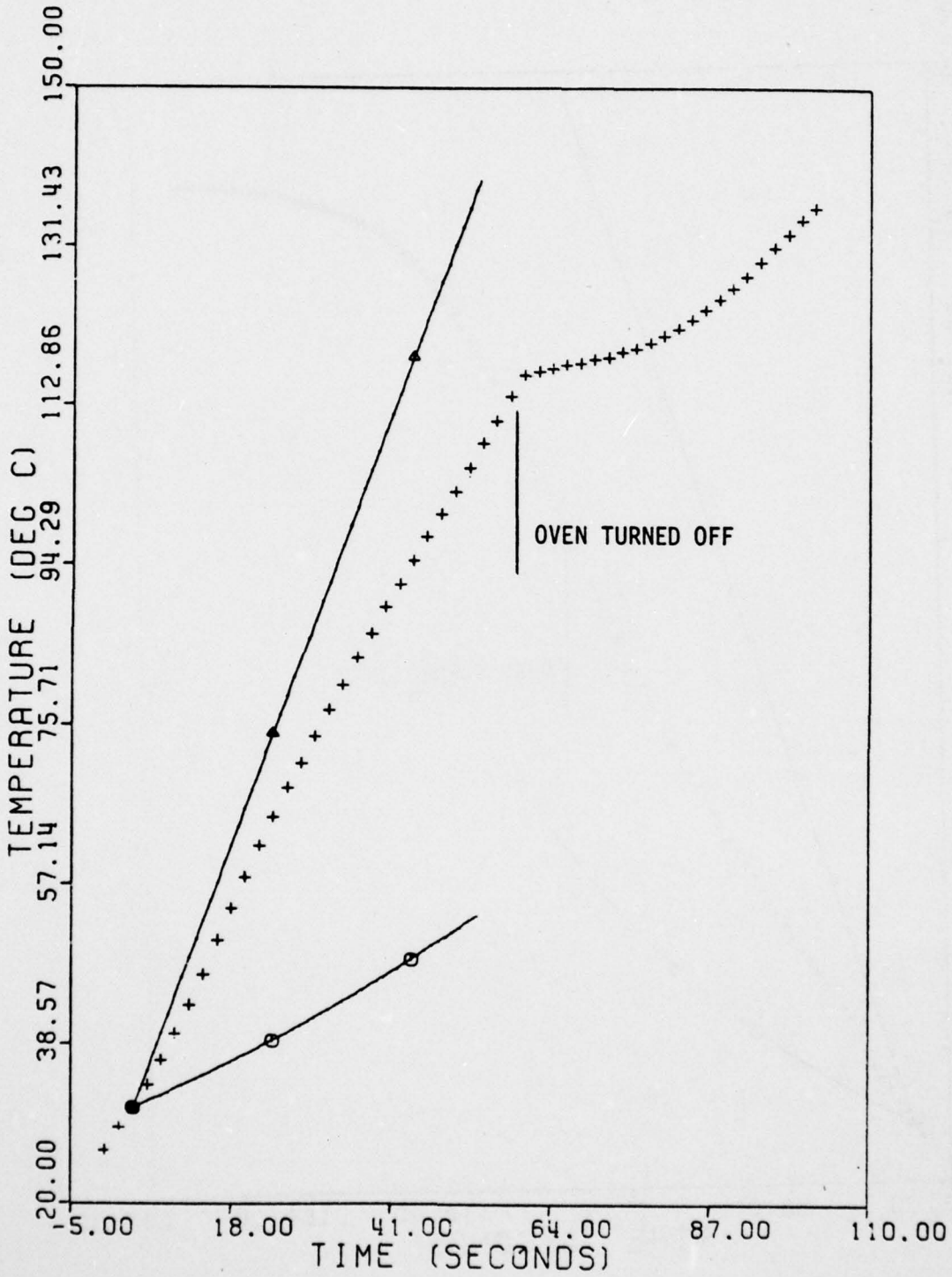


Figure 5-1: Experimental microwave heating in 30 ml of 828-T403 at 245 W and 2.45 GHz. Solid lines show models based on the loss tangent of gelled samples (θ) and pure water (Δ).

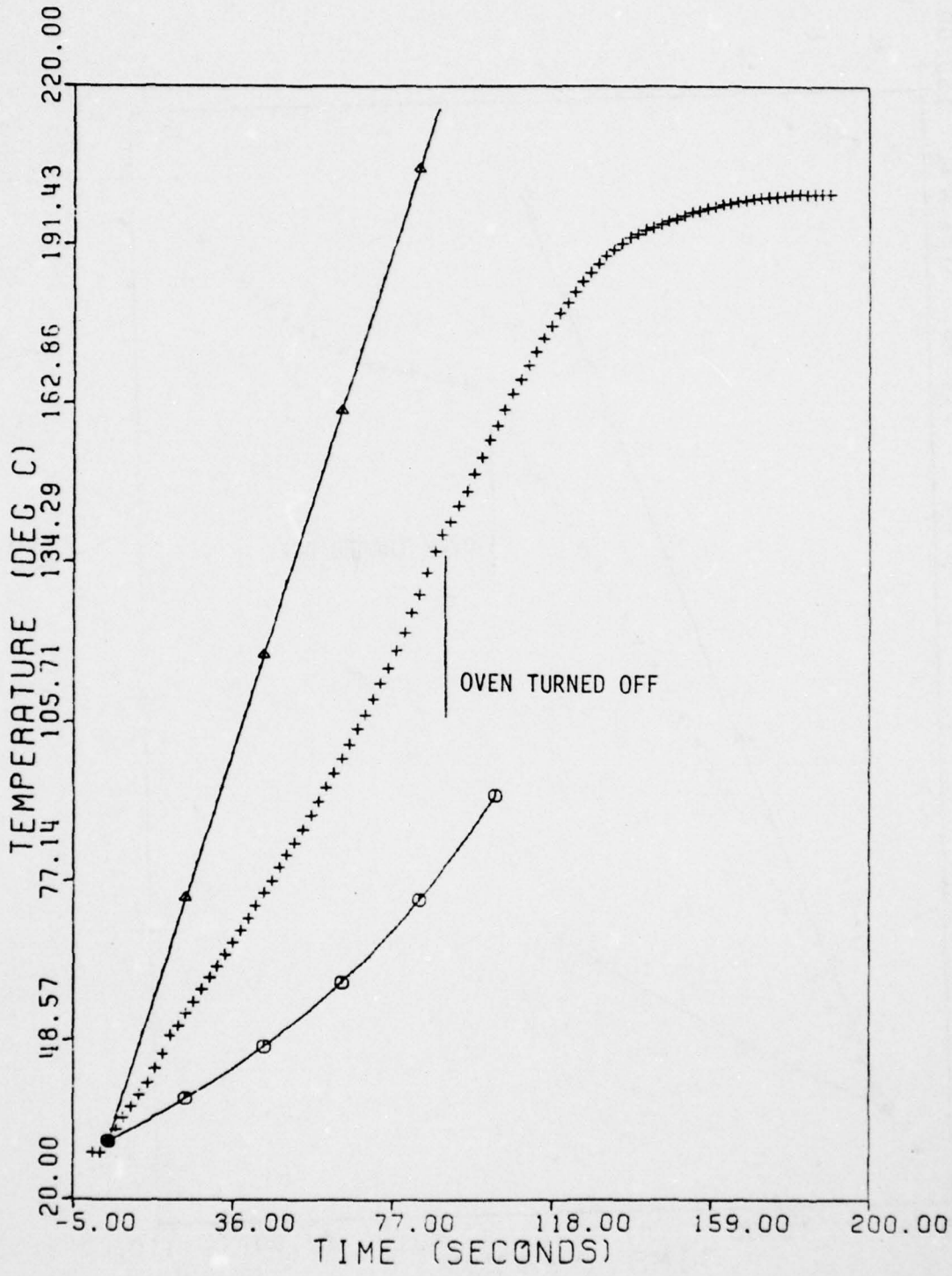


Figure 5-2: Experimental microwave heating in 30 ml 828-T403 at 245 W and 2.45 GHz. Solid lines show models based on the loss tangent of gelled samples (θ) and pure water (Δ).

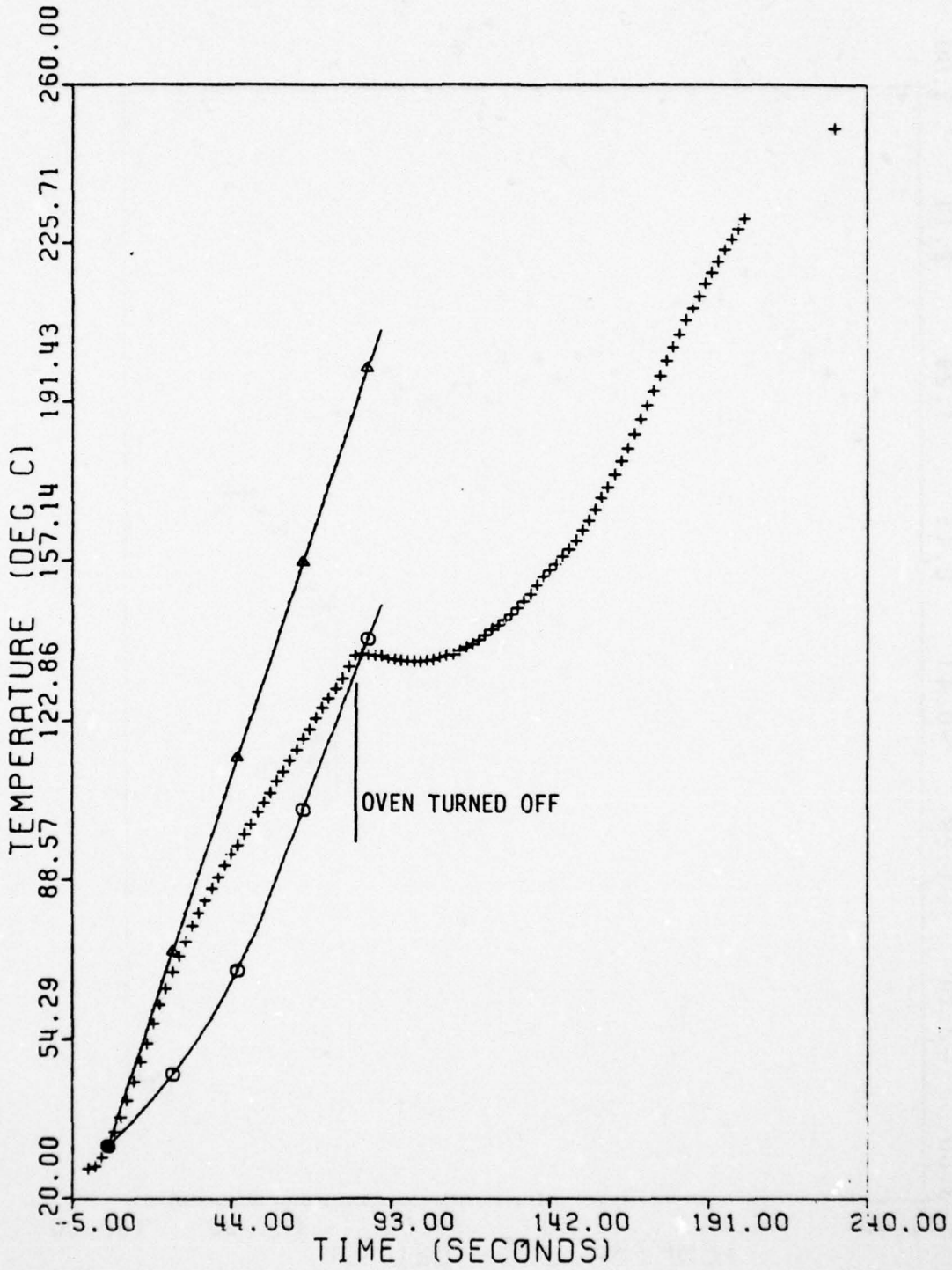


Figure 5-3: Experimental microwave heating in 30 ml 828-Z at 245 W and 2.45 GHz. Solid lines show models based on the loss tangent of gelled samples (θ) and pure water (Δ).

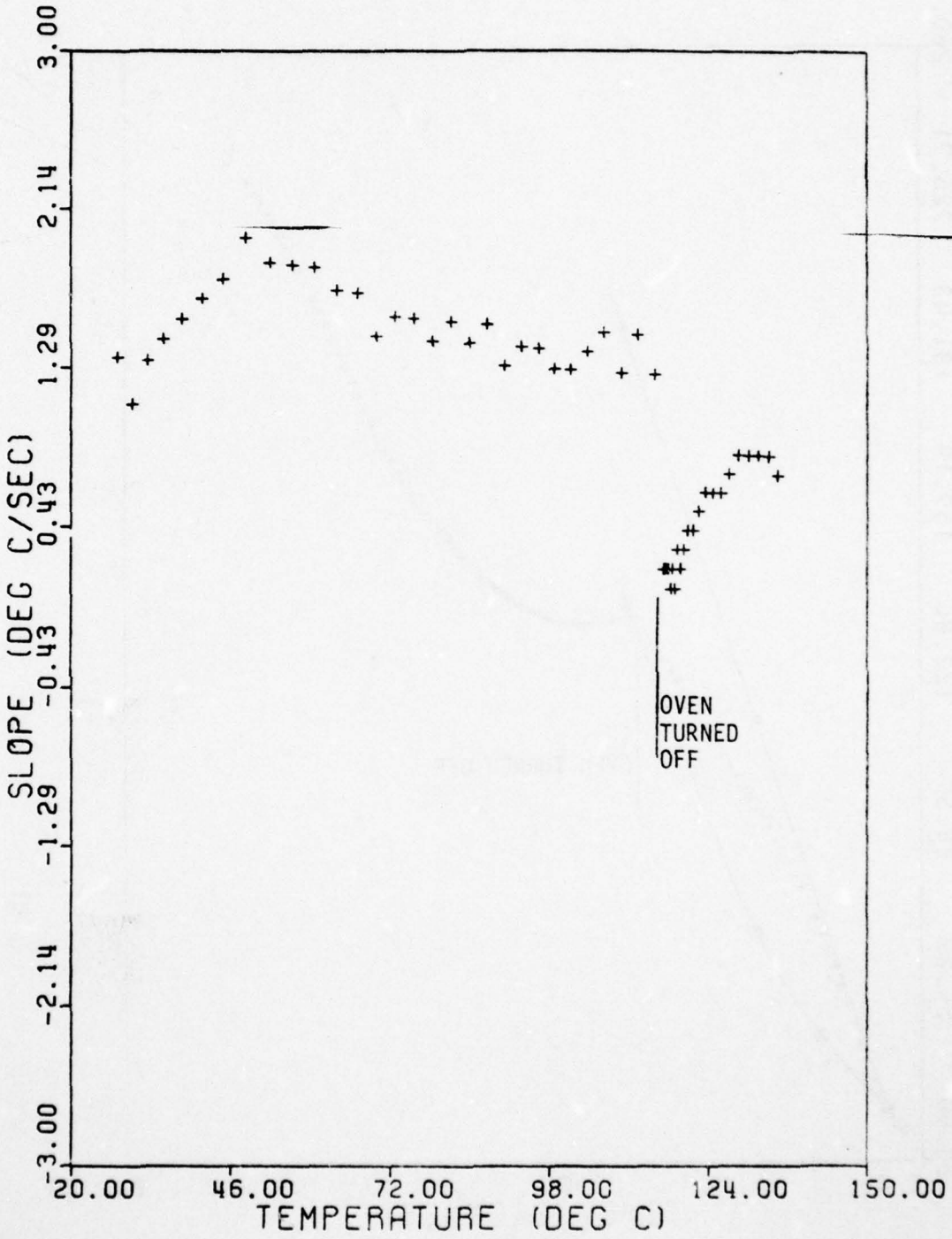


Figure 5-4: Slope of experimental heating curve from Figure 5-1 versus temperature.

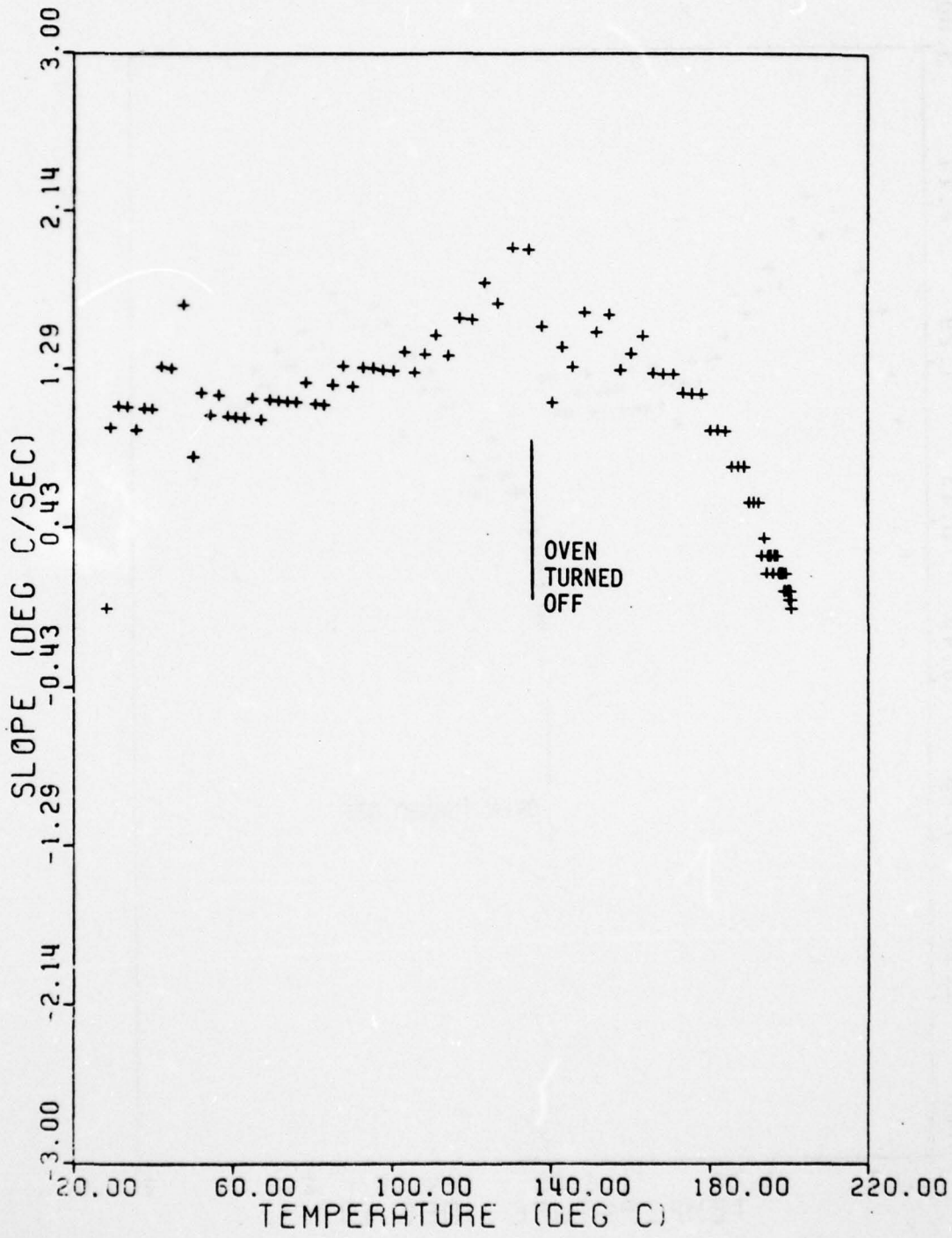


Figure 5-5: Slope of experimental heating curve from Figure 5-2 versus temperature.

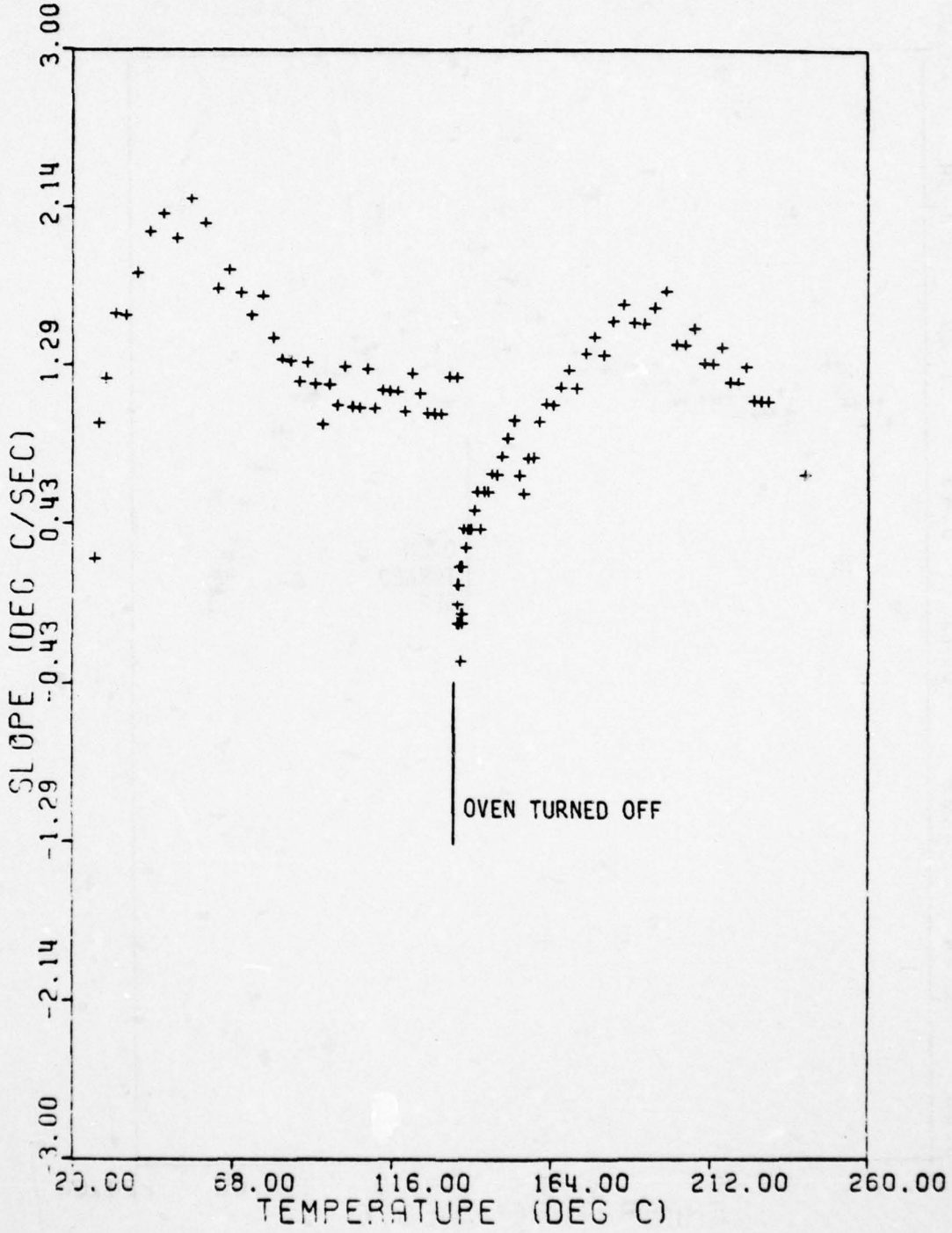


Figure 5-6: Slope of experimental heating curve from Figure 5-3 versus temperature.

the epoxy displayed the loss tangent of distilled water, given as

$$\tan \delta_{H_2O} = \frac{3.26}{T}$$

at 2.45 GHz [7]. It is obvious from the graphs that the loss tangent of the uncured epoxy is best described by that of distilled water. Figures 5-1 and 5-3 show excellent agreement with this model while Figure 5-2 suggests a loss tangent of intermediate value. The important aspect of this data is, however, that the shape of the experimental heating curve is best described by the model based on the loss tangent of water rather than that of the gelled epoxy reported in the previous chapter. The reasons for this unexpected microwave heating behavior and the deviations of experimental results from even this proposed model must now be examined.

In the analysis of a similar problem involving the microwave heating of wet wood, Voss [7] indicates that, based on the theory of mixed dielectrics, a mixture of water and a material with low loss and dielectric constant will exhibit a very large loss tangent and a low dielectric constant. Recall that the curing process in epoxies involves intermediate reactions whose byproducts include hydroxyl groups and water. The formation of these dipolar species during cure could result in the epoxy displaying a bulk loss tangent approaching that of pure water, while the bulk dielectric constant remains very low. Voss [7] also reports observations on low loss plastics showing the loss tangent of the bulk material to rapidly approach that of pure water. Thus it is concluded that, during cure, the microwave heating behavior of the epoxies is governed by a bulk loss tangent close to that of pure water

and a dielectric constant typical of the material. These effects result in a rate of heating much more rapid than that of water.

Although the observed microwave heating curves for the epoxy during cure generally agree with the proposed model, it is necessary to discuss anomalies in the data. Some deviation between experiment and theory may be due to errors inherent in the model for several reasons. For instance, the free space electric field in the cavity was determined experimentally and with the aid of simplifying assumptions. In addition, data for the specific heat as a function of sample temperature were not available. The best available value of 0.4 cal/gm$^{o}$C was used for this parameter. The model also assumes the ideal condition that full power of 245 watts is available for absorption by the sample. This is undoubtedly not the case due to impedance mismatch and losses inherent in the microwave oven itself. Also, there is no consideration for exchange of heat between the sample and the air in the cavity. These considerations result in experimental error that cannot be accounted for and undoubtedly result in some deviation of the model from the experimental curve.

The sources of error discussed above do not take into account the major sources of deviation between experiment and model. The model is in good agreement with the experimental results at the lower temperatures. At higher sample temperatures, however, the slope of the experimental curve decreases and the deviation from the model increases. This occurs at approximately 50$^{o}$C for the 828-T403 samples and 75$^{o}$C for the sample of 828-Z. It is proposed that some of the energy absorbed by the epoxy at these temperatures goes to promoting a chemical reaction rather than being lost as heat. This results in an observed decrease in the slope of

AD-A067 732 VANDERBILT UNIV NASHVILLE TN DEPT OF ELECTRICAL ENGI--ETC F/G 11/9
MICROWAVE CURING OF EPOXY RESINS.(U)
SEP 78 L K WILSON, J P SALERNO DAAG46-76-C-0035

UNCLASSIFIED USAAVRADCOM-TR-78-46 NL

2 OF 2
ADA
067732

END
DATE
FILMED
6-79
DDC

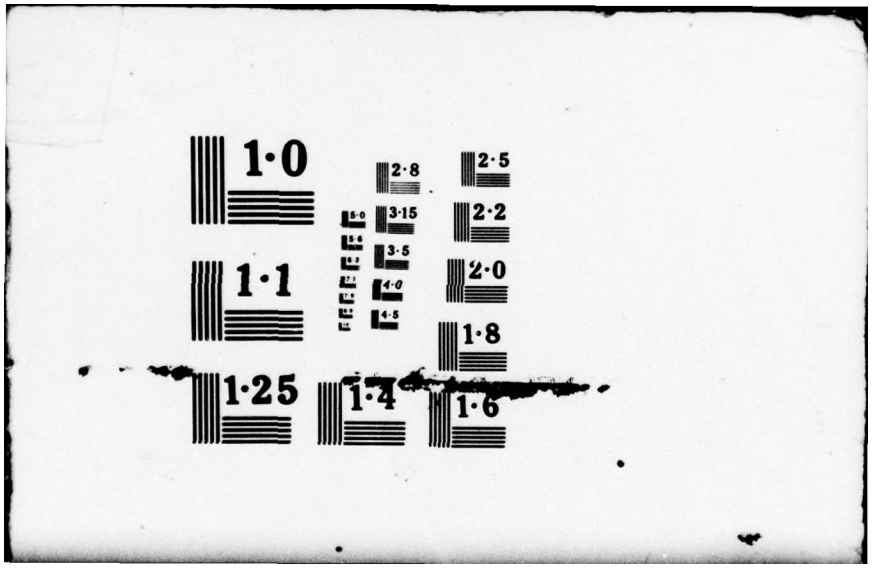
1·0
1·1
1·25
2·8
3·15
3·5
4·0
4·5
1·4
2·5
2·2
2·0
1·8
1·6

the heating curve. In addition, the increase in $\varepsilon_R'$ as the material cures, as discussed previously, may be partially responsible for this decrease in slope.

During these portions of the heating cycle, hydroxyl groups, and possibly even water, present in the original epoxy resin and produced as byproducts of intermediate reactions, effectively create a mixed dielectric and result in a bulk loss tangent close to that of pure water. At a certain temperature, it appears that an exothermic reaction becomes dominant and increases the sample temperature rather dramatically, eventually resulting in boiling. It is speculated that the large amount of energy absorbed by the epoxy in a relatively short period of time promotes a sequence of exothermic chemical reactions. These reactions proceed very rapidly, due to the large amount of available energy, resulting in a very large increase in temperature.

In summary, it is proposed that the microwave heating behavior of the epoxies is governed by a bulk loss tangent very close to that of pure water and a low dielectric constant as was determined by experiment. This results in very rapid heating of the material with large amounts of energy absorbed in a short period of time. As a result, the associated chemical reactions proceed rapidly and cause dramatic heating and solidification of the samples.

# CHAPTER VI

## CONCLUSIONS

This report has presented the results of an investigation of the mechanisms involved in microwave heating of epoxy systems in order to promote their cure. The purpose of this work concerns the possible application of this heating method to the curing of thick fiberglass/epoxy laminates. This chapter will summarize the material previously presented as it pertains to this application.

A discussion of the basic properties and chemistry of epoxy resins has been presented with special attention given to the chemical species pertinent to their interaction with the microwave field. It was noted that the curing reactions are generally quite complex and depend on the particular resin and curing agent under consideration. The main feature of interest is the presence of alcoholic hydroxyl groups in the original resins and the formation of additional hydroxyl groups, as alcohols or water molecules, during the curing process.

The concepts of dielectric polarization and complex permittivity, due to the action of a time dependent electric field on the material, were then developed. Since the effects of microwave frequency radiation on dipolar species in an amorphous material is of interest, Debye's theory of dielectric materials was presented. From these concepts, a relation for the rate of change in temperature of a dielectric sample experiencing an electric field was developed in terms of both material

and field dependent parameters.

Since the rate of microwave heating depends on the dielectric constant and loss tangent of the epoxies, it was necessary to measure these parameters as functions of both microwave frequency and sample temperature. These measurements were made on gelled samples of two epoxy systems and the results are presumed representative for all four epoxy systems under investigation. A technique for modeling the microwave heating behavior of the epoxies was developed from the derived relations. Experimental high power heating studies show best agreement with a model based on the assumption that the curing epoxies exhibit a bulk loss tangent close to that of pure water, rather than the value measured for the gelled epoxy, and a dielectric constant in the same range as that of the gelled material. This phenomena is attributed to the presence of hydroxyl groups in the material which effectively result in a mixed dielectric. Anomalies in the experimental heating curve are postulated as being due to the promotion of the chemical reactions involved in the cure.

The reasons for the significant difference between the measured values of the loss tangent and the values observed in high power heating experiments are not clear. The most plausible explanation is that the gelled samples used for the measurements exhibited dielectric properties representative of cured rather than uncured epoxy. Based on the experimental results and the related microwave heating studies cited, it is concluded that microwave heating in the uncured epoxies is due to energy absorption by dipolar hydroxyls resulting in extremely rapid heating. Since experiments indicate the uncured epoxies have a loss tangent close to that of pure water and a low dielectric constant given

by the experimental values, the depth of penetration in the curing epoxies, given by equation (III-21), has a minimum value of approximately 4 cm.

The work presented in this report leads to the conclusion that the use of microwave heating to promote the cure of thick fiberglass/epoxy laminate structures is a viable alternative to conventional methods. The depth of penetration of the electric field, as indicated by the observed dielectric properties of the pure epoxy, should be satisfactory for the uniform cure of the material. Although the problem of reflections caused by the laminate structure is not addressed in this report, it should be of little consequence if the thickness of each lamination is small compared to the wavelength of radiation. This condition should be satisfied at conventional microwave heating frequencies. If these reflections prove to be a problem, they could be reduced by matching the dielectric constants of the glass and epoxy. In practice, it would be necessary to control the heating process in order to prevent the thermal runaway shown in the high power heating experiments. This effect is believed to result from extremely rapid promotion of the exothermic curing reactions. It is speculated that the conclusions of this research are valid for all the epoxies of concern.

It may be possible to measure the dielectric properties of the epoxies as a function of degree of cure by infrared techniques. This data could be used to accurately predict the heating behavior for comparison with experiment. Such techniques and investigations were beyond the scope of this effort.

# APPENDIX I

## PROGRAM TEMPTHEORY

THIS PAGE IS BEST QUALITY PRACTICABLE
FROM COPY FURNISHED TO DDC

```
C
C
C     PROGRAM TEMPTHEORY
C
C     MODEL OF TEMPERATURE OF A DIELECTRIC SAMPLE HEATED
C     BY MICROWAVE RADIATION AT 2.45 GHZ.
C
C     ALOSS = LOSS TANGENT OF SAMPLE NORMALIZED TO ROOM TEMP.
C     EPR = RELATIVE DIELECTRIC CONST. OF SAMPLE (NORM. TO RM TEMP)
C     N = NUMBER OF DATA POINTS
C     DELTA = TIME INCREMENT BETWEEN EACH OF THE N POINTS
C     EPCON = ROOM TEMP RELATIVE DIELECTRIC CONST. OF SAMPLE
C     ALCON = ROOM TEMP LOSS TANGENT OF SAMPLE
C     INDEX = INCREMENT OF DATA POINTS OUTPUT
C     ESAMP = ELECTRIC FIELD AMPLITUDE IN SAMPLE
C
C     DC = RELATIVE DIELECTRIC CONST. AS A FUNCTION OF TEMP
C     ALT = LOSS TANGENT AS A FUNCTION OF TEMPERATURE
C
C     DCB:  F:1  I/O DEVICE
C           F:2  PLOT FILE
C
C
      DIMENSION TEMP(500),TIME(500)
      INTEGER YES,NO
      DATA YES,NO/4HY    ,4HN    /
      DATA EPO,PI,FREQ/8.854E-12,3.14159,2.45E09/
C
C     INITIALIZE PARAMETERS
C
      W=2.*PI*FREQ
5     WRITE(1,100)
      READ(1,101) EPCON,ALCON,AMASS,VOL,CV,PMAX
      IF(PMAX .EQ. 245.) EAIR=1.62E05
      IF(PMAX .EQ. 700.) EAIR=2.69E05
8     WRITE(1,108)
      READ(1,105) TEMP(1),TIME(1),DELTA,N
      TLIM=85.
C
C     COMPUTE TEMPERATURE/TIME CURVE
C
      X=0.2389*W*VOL*EPO/(2.*AMASS*CV)
      DO 12 I=2,N
      TIME(I)=TIME(1)+(I-1)*DELTA
      IF(TEMP(I-1) .LT. TLIM) GO TO 9
      CALL CALC(TLIM,EPR,ALOSS)
      GO TO 10
9     CALL CALC(TEMP(I-1),EPR,ALOSS)
10    DC=EPCON*EPR
      ALT=ALCON*ALOSS
      ESAMP=EAIR/DC
C
C     CHECK POWER LOSS
C
      PLOSS=W*EPO*DC*ALT*VOL*ESAMP*ESAMP
      IF(PLOSS .LE. PMAX) GO TO 12
      ESAMP=SQRT(PMAX/(W*EPO*DC*ALT*VOL))
12    TEMP(I)=X*DC*ALT*ESAMP*ESAMP*DELTA+TEMP(I-1)
```

THIS PAGE IS BEST QUALITY PRACTICABLE
FROM COPY FURNISHED TO DDC

```
C     OUTPUT COMPUTED DATA
C
      INDEX=4
      WRITE(1,103)
      WRITE(1,102) TIME(1),TEMP(1)
      J=1
20    J=J+INDEX
      IF(J .GE. N) GO TO 25
      WRITE(1,102) TIME(J),TEMP(J)
      GO TO 20
25    WRITE(1,102) TIME(N),TEMP(N)
C
C     BUILD PLOT FILE
C
      WRITE(1,106)
      READ(1,110) IPLOT
      IF(IPLOT .NE. YES) GO TO 38
      WRITE(1,109)
      READ(1,101) NUM
      INDEX=N/NUM
      WRITE(2,101) TIME(1),TEMP(1)
      J=1
      KOUNT=2
30    J=J+INDEX
      IF(J .GE. N) GO TO 35
      WRITE(2,101) TIME(J),TEMP(J)
      KOUNT=KOUNT+1
      GO TO 30
35    WRITE(2,101) TIME(N),TEMP(N)
      WRITE(2,101) KOUNT
C
C     CONCLUDE PROGRAM
C
38    WRITE(1,104)
      READ(1,110) ISTOP
      IF(ISTOP .EQ. YES) GO TO 40
      WRITE(1,107)
      READ(1,110) ISTOP
      IF(ISTOP .EQ. YES) GO TO 5
      GO TO 8
40    STOP
C
C     FORMATS
C
100   FORMAT(1HO,'INPUT:  RELATIVE DIELECTRIC CONSTANT'/9X,
     &'LOSS TANGENT'/9X,'SAMPLE MASS IN GRAMS'/9X,'SAMPLE VOLUME'
     &' IN CUBIC METERS'/9X,'SAMPLE SPECIFIC HEAT IN CAL/GRAM/'
     &'DEG C'/9X,'MAXIMUM POWER (245 OR 700) WATTS'/9X,'FORMAT('
     &'7G)')
101   FORMAT(6G)
102   FORMAT(F8.2,4X,F8.2)
103   FORMAT(1HO,'TIME (S)',3X,'TEMP (DEG C)')
104   FORMAT(1HO,'STOP? (Y/N)')
105   FORMAT(3G,1I)
106   FORMAT(1HO,'BUILD A PLOT FILE? (Y/N)')
107   FORMAT(1HO,'RESET SAMPLE PARAMETERS? (Y/N)')
108   FORMAT(1HO,'INPUT INITIAL TEMP AND TIME, TIME INCREMENT,'
     &,'TOTAL NO. OF DATA POINTS'/'FORMAT(3G,1I)')
109   FORMAT(1HO,'INPUT NO. OF POINTS TO BE PLOTTED')
110   FORMAT(A1)
      END
```

THIS PAGE IS BEST QUALITY PRACTICABLE
FROM COPY FURNISHED TO DDC

```
      SUBROUTINE CALC(T,EP,DELTA)
C
C
C     COMPUTES RELATIVE DIELECTRIC CONSTANT OF 828-T403
C     EPOXY (NORM. TO ROOM TEMP.) AND LOSS TANGENT OF PURE
C     WATER AT 2.45 GHZ.
C
C     EP = RELATIVE DIELECTRIC CONSTANT
C     DELTA = LOSS TANGENT
C     T = TEMPERATURE
C
C
      A4=5.30783E-08
      A3=-1.19546E-05
      A2=9.40779E-04
      A1=-2.89786E-02
      A0=1.30222
      EP=A4*T**4.+A3*T**3.+A2*T*T+A1*T+A0
      DELTA=3.26/T
      RETURN
      END
```

```
      SUBROUTINE CALC(T,EP,DELTA)
C
C
C     COMPUTES LOSS TANGENT AND RELATIVE DIELECTRIC CONSTANT
C     OF 828-T403 EPOXY AS A FUNCTION OF TEMPERATURE AT 2.45 GHZ.
C
C     EP = RELATIVE DIELECTRIC CONSTANT
C     DELTA = LOSS TANGENT
C     T = TEMPERATURE
C
C     VALUES OUTPUT ARE NORMALIZED TO THE ROOM TEMP. VALUE
C
C
      A4=5.30783E-08
      A3=-1.19546E-05
      A2=9.40779E-04
      A1=-2.89786E-02
      A0=1.30222
      EP=A4*T**4.+A3*T**3.+A2*T*T+A1*T+A0
      B2=2.69730E-07
      B1=1.85714E-05
      B0=4.68232E-04
      DELTA=B2*T*T+B1*T+B0
      DELTA=DELTA/0.0012
      RETURN
      END
```

# APPENDIX II

# PROGRAM SLOT2

THIS PAGE IS BEST QUALITY PRACTICABLE
FROM COPY FURNISHED TO DDC

```
C
C
C       PROGRAM SLOT2
C
C       COMPUTE DIELECTRIC CONSTANT AND LOSS FROM
C       COAXIAL SLOTTED LINE DATA
C
C       X = POSITION OF SHORTED MINIMUM TOWARD GEN
C       P1 = POSITION OF SHORTED MINIMUM TOWARD SHORT
C       P2 = POSITION OF MINIMUM P1 WITH LOADED LINE
C       VSWR = VSWR OF LOADED LINE
C
C       N = NUMBER OF DATA POINTS
C       ADATA = 60 CHARACTER ALPHANUMERIC LABEL
C       DIA = SAMPLE DIAMETER IN CM
C       T = SAMPLE THICKNESS IN CM
C       CORL = SAMPLE HOLDER LENGTH CORRECTION TERM
C
C
      DIMENSION ADATA(30)
      COMPLEX R,YL
      PI=3.14159
      READ(5,106) ADATA
      READ(5,100) DIA,T
      WRITE(1,104) ADATA
      READ(5,101) N
      CORL=1.98
      DO 50 I=1,N
      READ(5,102) X,P1,P2,VSWR
      WL=(P1-X)*2.
      FREQ=3.E10/WL*1.E-6
      YIN=VSWR
      BETA=2.*PI/WL*(P1-P2+CORL)
      C=SIN(BETA)
      D=COS(BETA)
      R=CMPLX(0.,C)
      YL=.02*(YIN*D-R)/(D-YIN*R)
      G=REAL(YL)
      B=AIMAG(YL)
      CAP=B/(2.*PI*FREQ*1.E06)*1.E12
      AREA=PI/4*DIA**2./10000.
      EP=B*T*1.E-8/(8.8542E-12*2.*PI*FREQ*AREA)+.0005
      TNDEL=G/B
   50 WRITE(1,105) FREQ,G,B,CAP,EP,TNDEL
  100 FORMAT(2F10.7)
  101 FORMAT(I3)
  102 FORMAT(4F10.3)
  104 FORMAT(1HO//,'DIELECTRIC PROPERTIES OF'//,5X,30A2,
     $///,'FREQUENCY',3X,'CONDUCTANCE',3X,'SUSCEPTANCE',3X,'CAPACITANCE'
     $,3X,'DIELECTRIC',5X,'LOSS',
     $/,2X,'(MHZ)',7X,'(MHOS)',9X,'(MHOS)',9X,'(PF)',8X,'CONSTANT',5X,'T
     $ANGENT'/)
  105 FORMAT(F7.1,E16.4,E14.4,F11.3,F13.3,E15.4)
  106 FORMAT(30A2)
      STOP
      END
```

## REFERENCES


1. "Microwaves Cure Urethane Car Seats", Chem. Eng. News, 41:50-52 (1963).

2. R. V. Decareau, "For Microwave Heating Tune to 915 Mc or 2450 Mc", Food Eng., 37:54-56(1965).

3. P. W. Crapuchettes, "Microwaves on the Production Line", Electronics, 39:123-130(1966).

4. S. Goldblith and W. E. Pace, "Some Considerations in the Processing of Potato Chips", J. Microwave Power, 2:95-98(1967).

5. J. B. Hasted and M. A. Shah, "Microwave Absorption by Water in Building Materials", Brit. J. Appl. Phys, 15:825-836(1964).

6. H. C. Warner, "Microwave Processing of Sheet Materials," J. Microwave Power, 1:81-88(1966).

7. W. G. A. Voss, "Factors Affecting the Operation of High-Power Microwave Heating Systems for Lumber Processing", IEEE Trans. Ind. Gen. Appl., IGA-2:234-243(1966).

8. J. P. Salerno, L. K. Wilson, and B. M. Halpin, "Application of Microwave Heating to the Curing of Fiberglass/Epoxy Laminates", in Proceedings of Southeastcon '77: IEEE Region 3 Conference 1977, pp. 504-506.

9. H. Lee and K. Neville, Epoxy Resins, New York: McGraw-Hill, 1957.

10. B. M. Halpin, private communication.

11. H. Lee and K. Neville, Handbook of Epoxy Resins, New York: McGraw-Hill, 1967.

12. H. Puschner, Heating With Microwaves, New York: Springer-Verlag, 1966.

13. A. R. von Hippel, Dielectrics and Waves, New York: Wiley, 1954, and references therein.

14. H. Frohlich, Theory of Dielectrics, London: Oxford University Press, 1958.

15. P. Debye, Polar Molecules, New York: Chemical Catalog Co., 1929.

16. K. S. Cole and R. H. Cole, "Dispersion and Absorption in Dielectrics," J. Chem. Phys., 9:341-351(1941).

17. L. Onsager, "Electric Moments of Molecules and Liquids," J. Am. Chem. Soc., 58:1486-1493(1936).

18. R. F. Field, "Lumped Circuits," in Dielectric Materials and Applications, A. R. von Hippel, Ed., New York: Wiley, 1954, pp. 47-62.

19. J. D. Pearson, "U. H. F. and Microwave Dielectric Properties of a Class of Amorphous Semiconductors," M. S. Thesis, Vanderbilt University, 1972.

20. W. H. Hayt, Jr., Engineering Electromagnetics, 2 ed., New York: McGraw-Hill, 1967.

21. W. B. Westphal, "Distributed Circuits," in Dielectric Materials and Applications, A. R. von Hippel, Ed., New York: Wiley, 1954, pp. 63-87.

22. H. E. Bussey, "Measurement of RF Properties of Materials--A Survey," Proceedings of the IEEE, 55:1046-1053(1967).

23. D. A. Daley et al., "Lumped Elements in Microwave Integrated Circuits," IEEE Trans. Microwave Theory Tech., MTT-15:713-721(1967).

24. C. R. James, W. Tinga, and W. G. A. Voss, "Some Factors Affecting Energy Conversion in a Microwave Cavity," J. Microwave Power, 1:97-107(1966).

25. R. H. Bolt, "Frequency Distribution of Eigentones in a Three-Dimensional Continuum," J. Acous. Soc. Am., 10:228-234(1939).

26. D. Y. Maa, "Distribution of Eigentones in a Rectangular Chamber at Low Frequency Range," J. Acous. Soc. Am., 10:235-238(1939).

27. C. Morin, "Multimode Cavities for Industrial Microwave Processing," Electron. Communicator, 1:15(1966).

Army Materials and Mechanics Research Center
Watertown, Massachusetts 02172
Microwave Curing of Epoxy Resins
L. K. Wilson and J. P. Salerno,
Electrical Engineering Department
Vanderbilt University
Nashville, Tennessee 37235
Technical Report AVRADCOM TR 78-46, September 1978
99 pp. illus. tables. Contract DAAG46-76-C-0035,
D/A Project 1737042, AMCMS Code 1497.94.5.S7042

Final Report

The objective of this researchprogram was to investigate the fundamental mechanisms responsible for microwave heating of epoxy resins as applied to curing of fiberglass/epoxy laminate structures. Microwave dielectric properties of gelled samples were measured. A theoretical model for heating was compared to experimental heating data at 2.45 GHz with good agreement. It is concluded that the use of microwave heating to enhance curing of thick fiberglass/epoxy structures is a viable alternative to conventional methods.

AD _____

UNCLASSIFIED
UNLIMINTED DISTRIBUTION

Key Words

Epoxy Resins
Curing
Dielectric Properties
Dielectric Heating
Microwaves

Army Materials and Mechanics Research Center
Watertown, Massachusetts 02172
Microwave Curing of Epoxy Resins
L. K. Wilson and J. P. Salerno,
Electrical Engineering Department
Vanderbilt University
Nashville, Tennessee 37235
Technical Report AVRADCOM TR 78-46, September 1978
99 pp. illus. tables. Contract DAAG46-76-C-0035,
D/A Project 1737042, AMCMS Code 1497.94.5.S7042

Final Report

The objective of this researchprogram was to investigate the fundamental mechanisms responsible for microwave heating of epoxy resins as applied to curing of fiberglass/epoxy laminate structures. Microwave dielectric properties of gelled samples were measured. A theoretical model for heating was compared to experimental heating data at 2.45 GHz with good agreement. It is concluded that the use of microwave heating to enhance curing of thick fiberglass/epoxy structures is a viable alternative to conventional methods.

AD _____

UNCLASSIFIED
UNLIMINTED DISTRIBUTION

Key Words

Epoxy Resins
Curing
Dielectric Properties
Dielectric Heating
Microwaves

Army Materials and Mechanics Research Center
Watertown, Massachusetts 02172
Microwave Curing of Epoxy Resins
L. K. Wilson and J. P. Salerno,
Electrical Engineering Department
Vanderbilt University
Nashville, Tennessee 37235
Technical Report AVRADCOM TR 78-46, September 1978
99 pp. illus. tables. Contract DAAG46-76-C-0035,
D/A Project 1737042, AMCMS Code 1497.94.5.S7042

Final Report

The objective of this researchprogram was to investigate the fundamental mechanisms responsible for microwave heating of epoxy resins as applied to curing of fiberglass/epoxy laminate structures. Microwave dielectric properties of gelled samples were measured. A theoretical model for heating was compared to experimental heating data at 2.45 GHz with good agreement. It is concluded that the use of microwave heating to enhance curing of thick fiberglass/epoxy structures is a viable alternative to conventional methods.

AD _____

UNCLASSIFIED
UNLIMINTED DISTRIBUTION

Key Words

Epoxy Resins
Curing
Dielectric Properties
Dielectric Heating
Microwaves

Army Materials and Mechanics Research Center
Watertown, Massachusetts 02172
Microwave Curing of Epoxy Resins
L. K. Wilson and J. P. Salerno,
Electrical Engineering Department
Vanderbilt University
Nashville, Tennessee 37235
Technical Report AVRADCOM TR 78-46, September 1978
99 pp. illus. tables. Contract DAAG46-76-C-0035,
D/A Project 1737042, AMCMS Code 1497.94.5.S7042

Final Report

The objective of this researchprogram was to investigate the fundamental mechanisms responsible for microwave heating of epoxy resins as applied to curing of fiberglass/epoxy laminate structures. Microwave dielectric properties of gelled samples were measured. A theoretical model for heating was compared to experimental heating data at 2.45 GHz with good agreement. It is concluded that the use of microwave heating to enhance curing of thick fiberglass/epoxy structures is a viable alternative to conventional methods.

AD _____

UNCLASSIFIED
UNLIMINTED DISTRIBUTION

Key Words

Epoxy Resins
Curing
Dielectric Properties
Dielectric Heating
Microwaves

DISTRIBUTION LIST
US ARMY AVIATION RESEARCH AND DEVELOPMENT COMMAND
MANUFACTURING TECHNOLOGY (MANTECH) PROJECTS
FINAL OR INTERIM REPORTS

| No. of Copies | To |
|---|---|
| | Commander; US Army Aviation Research and Development Command<br>P. O. Box 209: St. Louis, MO 63166 |
| 10 | ATTN: DRDAV-EXT |
| 1 | ATTN: DRDAV-EQ |
| 1 | Project Manager; Advanced Attack Helicopter;<br>ATTN: DRCPM-AAH-TM; P. O. Box 209; St. Louis, MO 63166 |
| 1 | Project Manager; Black Hawk; ATTN: DRCPM-BH-T; P. O. Box 209;<br>St. Louis, MO 63166 |
| 1 | Project Manager; CH-47 Modernization; ATTN: DRCPM-CH47M-T;<br>P. O. Box 209; St. Louis, MO 63166 |
| 1 | Project Manager; Aircraft Survivability Equipment;<br>ATTN: DRCPM-ASE-TM; P. O. Box 209; St. Louis, MO 63166 |
| 1 | Project Manager; Cobra; ATTN: DRCPM-CO-T; P. O. Box 209;<br>St. Louis, MO 63166 |
| 1 | Project Manager; Iranian Aircraft Program; ATTN: DRCPM-IAP-T;<br>P. O. Box 209; St. Louis, MO 63166 |
| 4 | Commander; US Army Material Development and Readiness Command;<br>ATTN: DRCMT; 5001 Eisenhower Avenue; Alexandria, VA 22333 |
| 1 | Director; Applied Technology Laboratory; Research and<br>Technology Laboratories (AVRADCOM); ATTN: DAVDL-EU-TAS;<br>Ft. Eustis, VA 23604 |
| 1 | Director; Aeromechanics Laboratory; Research and Technology<br>Laboratories (AVRADCOM); ATTN: DAVDL-AM; Mail Stop 215-1;<br>Moffett Field, CA 94035 |
| 1 | Director; Structures Laboratory; Research and Technology<br>Laboratories (AVRADCOM); ATTN: DAVDL-LA; Mail Stop 266;<br>Hampton, VA 23365 |
| 1 | Project Manager; Navigation/Control Systems; ATTN: DRCPM-NE-TM;<br>Ft. Monmouth, NJ 07703 |
| 1 | Commander; Avionics Research and Development Activity;<br>ATTN: DAVAA-O; Ft. Monmouth, NJ 07703 |
| 1 | Director; Propulsion Laboratory; Research & Technology<br>Laboratories (AVRADCOM); ATTN: DAVDL-LE; Mail Stop 77-5;<br>21000 Brook Park Rd; Cleveland, OH 44135 |

| No. of Copies | To |
|---|---|
| 1 | Director; US Army Materials & Mechanics Research Center; Watertown, MA 02172; ATTN: DRXMR-PT |
| 20 | ATTN: DRXMR-RD |
| 1 | Director; US Army Industrial Base Engineering Activity; Rock Island Arsenal; ATTN: DRXIB-MT; Rock Island, IL 61201 |
| | Air Force Materials Laboratory; Manufacturing Technology Division; Wright-Patterson Air Force Base, Ohio 45433 |
| 1 | ATTN: AFML/LTM |
| 1 | ATTN: AFML/LTN |
| 1 | ATTN: AFML/LTE |
| 1 | Commander; US Army Electronics Command; Ft. Monmouth, NJ ATTN: DRSEL-RD-P |
| 1 | Commander; US Army Missile Command; Redstone Arsenal, AL 35809 ATTN: DRSMI-IIE |
| | Commander; US Army Troop Support and Aviation Material Readiness Command; 4300 Goodfellow Blvd.; St. Louis, MO 63120 |
| 1 | ATTN: DRSTS-PLC |
| 1 | ATTN: DRSTS-ME |
| 2 | ATTN: DRSTS-DIL |
| 1 | Commander; US Army Armament Command; Rock Island, IL 61201 ATTN: DRSAR-PPR-1W |
| 1 | Commander; US Army Tank-Automotive Command; Warren, MI 48090 ATTN: DRSTA-RCM.1 |
| 12 | Commander; Defense Documentation Center; Cameron Station; Building 5; 5010 Duke Street; Alexandria, Virginia 22314 |
| 2 | Hughes Helicopter; Division of Summa Corporation; ATTN: Mr. R. E. Moore, Bldg. 314; M/S T-419; Centinella Avenue & Teale Street; Culver City, CA 90230 |
| 2 | Sikorsky Aircraft Division; United Aircraft Corporation; ATTN: Mr. Stan Silverstein; Section Supv. Manufacturing Tech; Stratford, Connecticut 06497 |
| 2 | Bell Helicopter Textron; Division of Textron, Inc.; ATTN: Mr. P. Baumgartner, Chief, Manufacturing Technology; P. O. Box 482; Ft. Worth, Texas 76101 |
| 2 | Kaman Aerospace Corp.; ATTN: Mr. A. S. Falcone, Chief of Materials Engineering; Bloomfield, Connecticut 06002 |

| No. of Copies | To |
|---|---|
| 2 | Boeing Vertol Company; ATTN: R. Pinckney, Manufacturing Technology; Box 16858; Philadelphia, PA 19142 |
| 2 | Detroit Diesel Allison Division, General Motors Corporation; ATTN: James E. Knott; General Manager; P. O. Box 894; Indianapolis, Ind. 46206 |
| 2 | General Electric Company; ATTN: Mr. H. Franzen; 10449 St. Charles Rock Road; St. Ann, MO 63074 |
| 2 | AVCO-Lycoming Corp; ATTN: Mr. V. Strautman, Manager Process Technology Laboratory; 550 South Main Street; Stratford, Conn. 08497 |
| 2 | United Technologies Corp.; Pratt & Whitney Aircraft Div.; Manufacturing Research and Development; ATTN: Mr. Ray Traynor; East Hartford, Conn. 06108 |
| 2 | Grumman Aerospace Corporation; ATTN: Richard Cyphers Manager, Manufacturing Technology, Plant 2, Bethpage, NY 11714 |
| 2 | ATTN: Albert Grenci, Manufacturing Engineer, Dept. 231 Plant 2, Bethpage, NY 11714 |
| 2 | Boeing Vertol Company; ATTN: R. Drago, Advanced Drive Systems Technology; P. O. Box 16858; Philadelphia, PA 19142 |
| 2 | Lockheed Missiles & Space Co., Inc.; ATTN: H. Dorfman; Research Specialist; Manufacturing Research; 1111 Lockheed Way; Sunnyvale, CA 94088 |